iScience

CellPress
OPEN ACCESS

Article

Kuragel: A biomimetic hydrogel scaffold designed to promote corneal regeneration

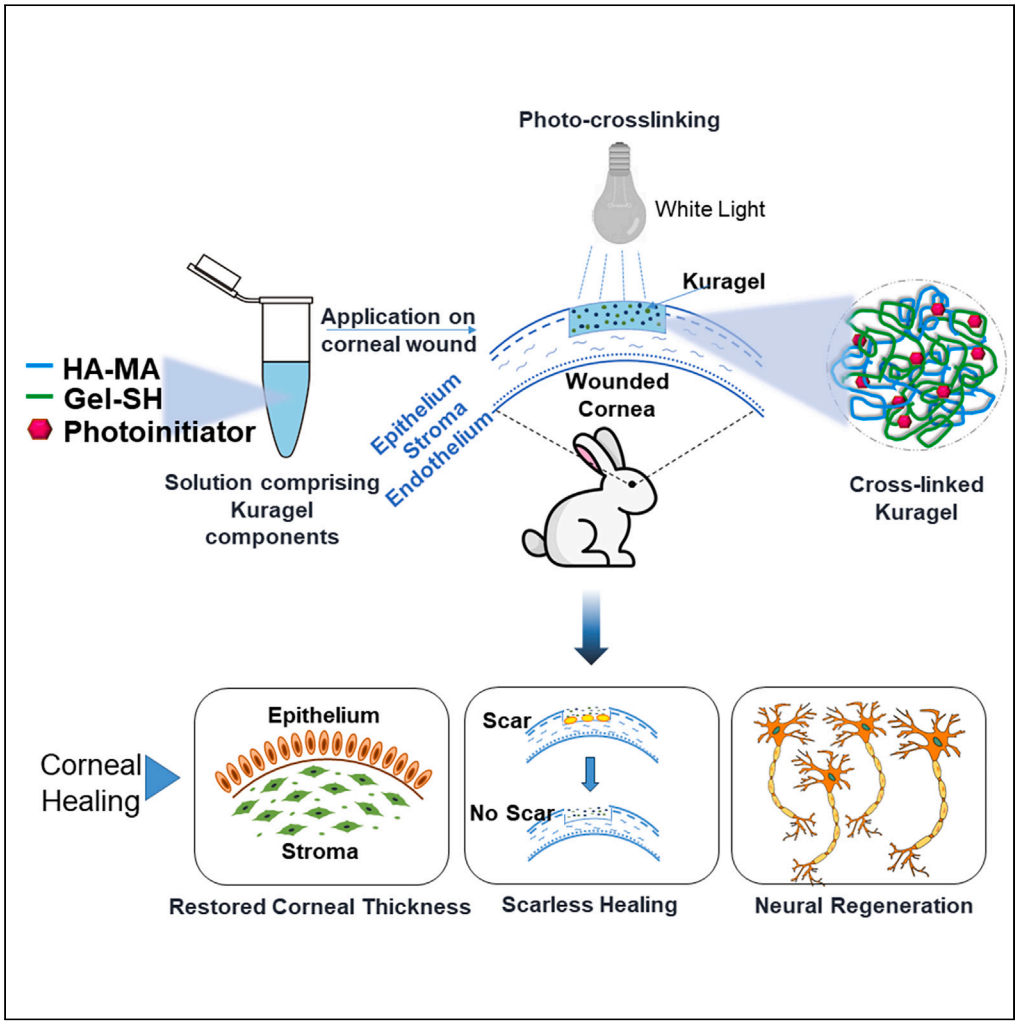

Parinita Agrawal, Anil Tiwari, Suvro Kanti Chowdhury, ..., Arun Chandru, Virender S. Sangwan, Tuhin Bhowmick

tuhin@pandorumtechnologies.in

Highlights

Photo-crosslinkable hydrogel, Kuragel prepared using gelatin and hyaluronic acid

Kuragel exhibits cornea mimetic optical, mechanical property, and biological support

Kuragel, an ideal sacrificial matrix offers sutureless application and bioadhesion

Cornea regeneration in rabbits by re-epithelialization, stroma, and nerve formation

Agrawal et al., iScience 27, 109641
May 17, 2024
Published by Elsevier Inc.
https://doi.org/10.1016/j.isci.2024.109641

iScience

CellPress
OPEN ACCESS

Article

Kuragel: A biomimetic hydrogel scaffold designed to promote corneal regeneration

Parinita Agrawal,[1] Anil Tiwari,[1,2] Suvro Kanti Chowdhury,[1] Mehak Vohra,[1] Abha Gour,[1,2] Neha Waghmare,[1] Utkarsh Bhutani,[1] S. Kamalnath,[1] Bharti Sangwan,[1] Jyoti Rajput,[1] Ritu Raj,[1] Nisha P. Rajendran,[1] Ajith V. Kamath,[1] Ramez Haddadin,[3] Arun Chandru,[1] Virender S. Sangwan,[2] and Tuhin Bhowmick[1,4,5,*]

SUMMARY

Cornea-related injuries are the most common cause of blindness worldwide. Transplantation remains the primary approach for addressing corneal blindness, though the demand for donor corneas outmatches the supply by millions. Tissue adhesives employed to seal corneal wounds have shown inefficient healing and incomplete vision restoration. We have developed a biodegradable hydrogel – Kuragel, with the ability to promote corneal regeneration. Functionalized gelatin and hyaluronic acid form photo-crosslinkable hydrogel with transparency and compressive modulus similar to healthy human cornea. Kuragel composition was tuned to achieve sufficient adhesive strength for sutureless integration to host tissue, with minimal swelling post-administration. Studies in the New Zealand rabbit mechanical injury model affecting corneal epithelium and stroma demonstrate that Kuragel efficiently promotes re-epithelialization within 1 month of administration, while stroma and sub-basal nerve plexus regenerate within 3 months. We propose Kuragel as a regenerative treatment for patients suffering from corneal defects including thinning, by restoration of transparency and thickness.

INTRODUCTION

Corneal defect, one of the major reasons catering to the occlusion of vision, hampers the refraction of light through the lens thereby culminating in partial or total blindness. Around 28 million people are affected with cornea blindness worldwide with 1.5 million cases getting added every year.[1] Untreated corneal injuries lead to scarring and thinning, ultimately aiding in permanent visual impairment. Corneal wounds resulting from microbial infections and autoimmune or ocular surface diseases can prove to be fatal if left unattended.[2] Current treatment modalities involve tissue adhesives such as cyanoacrylate, fibrin glue, polyethylene glycol (PEG)-based adhesives (ReSure and OcuSeal), and lamellar keratoplasty.[2,3] However, various disadvantages associated with them have encouraged the emerging need for evaluating hydrogels as an alternative that closely mimics the corneal stroma. An ideal hydrogel substitute should be cornea mimetic in terms of transparency and mechanical properties. In order to get well integrated with the underlying host tissue, it should have appropriate adhesive strength and cyto-compatibility, besides being biodegradable.

A wide range of natural and synthetic hydrogels incorporating gelatin,[4,5] collagen,[6,7] chitosan,[8,9] PEG,[10,11] and hyaluronic acid (HA)[6,12,13] have been studied for treating corneal defects. Recently, light-responsive and thermo-responsive hydrogels have gained prominence among researchers for corneal tissue engineering applications.[14] Photo-crosslinkable gelatin-based hydrogels exhibited effective healing in a rabbit stromal defect model thereby acting as sutureless alternatives to corneal transplantation.[3] Hydrogels from decellularized human cornea extracellular matrix (ECM) have shown significant improvement in the healing of corneal epithelial and stromal wounds.[15] They provided appropriate regenerative cues to the damaged microenvironment apart from being biocompatible, non-irritable, and non-mutagenic, though the dependency on donor cornea tissue for the extraction of ECM limits their widespread use and requires an ECM mimetic substitute.

Collagen and its derivatives, being biocompatible, have been the choice of researchers for a long time in developing hydrogels. Collagen-like peptides attached to PEG have demonstrated their efficiency as a viable alternative for full-length recombinant collagen in enhancing corneal regeneration in a miniature pig model.[16] These peptide derivatives facilitated their pro-regenerative effects by inducing generation of extracellular vesicles by the body's own host cells that migrated into the implants.[16] When mixed with fibrinogen, these peptides (termed LiQD Cornea) were shown to help in full-thickness corneal perforation.[17] Other studies have used collagen-based hydrogels for providing a regenerative solution for keratectomy wounds in epithelial and stromal regeneration.[7,18–20] Gelatin, being a hydrolyzed form of collagen,

[1]Pandorum Technologies Pvt., Ltd, Bangalore, India
[2]Dr. Shroff's Charity Eye Hospital, New Delhi, India
[3]Feinberg School of Medicine Northwestern University, Chicago, IL, USA
[4]Pandorum International Inc, San Francisco, CA, USA
[5]Lead contact
*Correspondence: tuhin@pandorumtechnologies.in
https://doi.org/10.1016/j.isci.2024.109641

shows lower immunogenicity and better aqueous solubility that makes it an excellent base biomaterial for ocular tissue engineering applications.[21] Crosslinked gelatin-based substitutes have also been employed as bioadhesives and cell-sheet carriers in addition to being used as scaffolds for aiding ocular repair.[3,22,23] A group of researchers showed glycidyl methacrylate-modified gelatin (Gel-MA) backbone makes the polymer crosslink in visible light, obtaining elastic hydrogel which is best suitable to be used as a bioadhesive for ocular applications.[23] Photo-crosslinkable hepatocyte growth factor (HGF)-loaded Gel-MA hydrogels have been shown to improve corneal epithelialization through sustained release of HGF for a month in porcine corneal defect models.[24] Gelatin has been widely acknowledged to promote cell adhesion and proliferation, facilitating corneal healing.[25–27] Gelatin contains cell adhesive RGD (arginine-glycine-aspartic acid) motifs as well as MMP cleavable sites facilitating cell proliferation and ECM remodeling, respectively.[25,27,28]

HA is a naturally occurring anionic, non-sulfated glycosaminoglycan that holds superior transparency and water-retention capabilities.[28–30] Apart from being highly tunable and biocompatible, its viscoelastic nature confers lubrication abilities beneficial for tear film maintenance.[30,31] Owing to its mucoadhesive property, HA has been utilized for constructing corneal epithelial cell-encapsulated supramolecular hydrogels for treating corneal wounds.[32] The HA-based hydrogels have been extensively studied for the treatment of corneal defects,[33,34] corneal re-epithelialization,[35] and bacterial keratitis treatments.[36] However, HA alone has a very short residence time,[32,33] where functionalization of HA with chemical groups such as methacrylic anhydride has demonstrated improved structural stability resulting in a photo-responsive material that can be crosslinked to obtain a stable hydrogel.[33,34]

Corneal crosslinking is an established procedure where riboflavin-mediated UV-A exposure leads to stromal collagen crosslinks giving stiffness to corneal stroma. It has been employed for the treatment of disorders involving corneal thinning like keratoconus, post-LASIK ectasia, and pellucid marginal degeneration.[37] Such an approach can be easily adapted in corneal tissue engineering by using functionalized biopolymers, which would provide control over the properties of *in situ* crosslinked matrix. The photo-crosslinkable biopolymers can be prepared by introducing methacryloyl and thiol groups in their chains. Photo-crosslinkable collagen derivatives employ chain growth polymerization crosslinking which gives a hydrogel that remains stable in the physiological condition for a longer duration.[38,39]

Visible light-initiated crosslinking system such as Eosin Y (absorption peak at 515 nm) has been explored in biomedical applications mainly for tissue engineering applications and proved to be non-toxic and biocompatible.[40] Eosin Y is known as a type II or non-cleavage type photoinitiator that, in the presence of triethanolamine (TEOA) as a co-initiator, can be activated via visible light to generate free radicals for polymerization.[41,42] Sani et al. have used Gel-MA-based, eosin-TEOA, and visible light crosslinked hydrogels and have shown their suitability for cornea tissue regeneration.[3] In this study, we developed a hydrogel system, Kuragel, that incorporates thiolated gelatin (Gel-SH) and methacrylated hyaluronic acid (HA-MA) with Eosin Y-TEOA as a photoinitiator. We also evaluated their physical properties and biocompatibility *in vitro* using corneal stromal cells and in a rabbit corneal wound model to demonstrate their suitability for corneal wound healing application.

While biopolymers have made significant advancements in regenerative medicine, addressing the challenge of optimizing their properties for long-term stability and developing scalable manufacturing processes remains crucial.[43,44] The bioengineering of these biopolymers holds significant potential in corneal wound healing. Since these biopolymers are derived from living organisms (plants, microbes, etc.), they inherently have properties that can be bioengineered and tweaked to meet a specific regenerative potential. Since these are naturally derived, they are very well tolerated and integrated with the surrounding human tissue. These are biodegradable, i.e., they are degraded and absorbed by the body over time and the biopolymer scaffold is gradually replaced by the native tissue. Moreover, this innovative approach of bioengineering has empowered researchers with unprecedented control over the rate of their degradation, opening up new possibilities for tailored regenerative applications.[45] Since our research deals with functionalized biopolymers (HA-MA and Gel-SH), bioengineering of these polymers has been carefully thought of to meet the target properties of the native corneal tissue. The functionalization allows immense control over the fabricated photo-crosslinkable hydrogels and is a great example of the customizability of the native biopolymers. The cutting-edge bioengineering of biopolymers for corneal wound healing represents an exciting avenue for research holding the promise of transforming the way corneal injuries and diseases are treated presently.

RESULTS

Material characterization

The biopolymers used in this study were functionalized to make them photoresponsive and obtain hydrogels with tunable properties. The functionalization of biopolymers HA-MA and Gel-SH was evaluated by ^{1}H-NMR and biochemical characterization.

^{1}H-NMR of the biopolymers

^{1}H-NMR was performed to identify the presence of methacryloyl groups in HA-MA using base HA polymer and thiol groups in Gel-SH using base gelatin polymer (Figure 1). On comparing the ^{1}H-NMR spectra of HA and HA-MA, two peaks were observed near 5.6 ppm (d) and 6.0 ppm (e) in HA-MA, which attribute to the functionalized methacryloyl group.[3] A similar comparison of ^{1}H-NMR spectra of gelatin and Gel-SH resulted in peaks at 2.56 (b) and 2.72 (c) ppm confirming the presence of thiol groups. These peaks correspond to the methylene next to the thiol groups.[46,47]

Biochemical assessment of thiol functionalization

Ellman's reagent, also known as 5,5′-dithio-bis-(2-nitrobenzoic acid) (DTNB), is used for assessing sulfhydryl groups (-SH or thiol) in a given sample. When DTNB comes into contact with a free sulfhydryl group, it forms a mixed disulfide along with 2-nitro-5-thiobenzoic acid

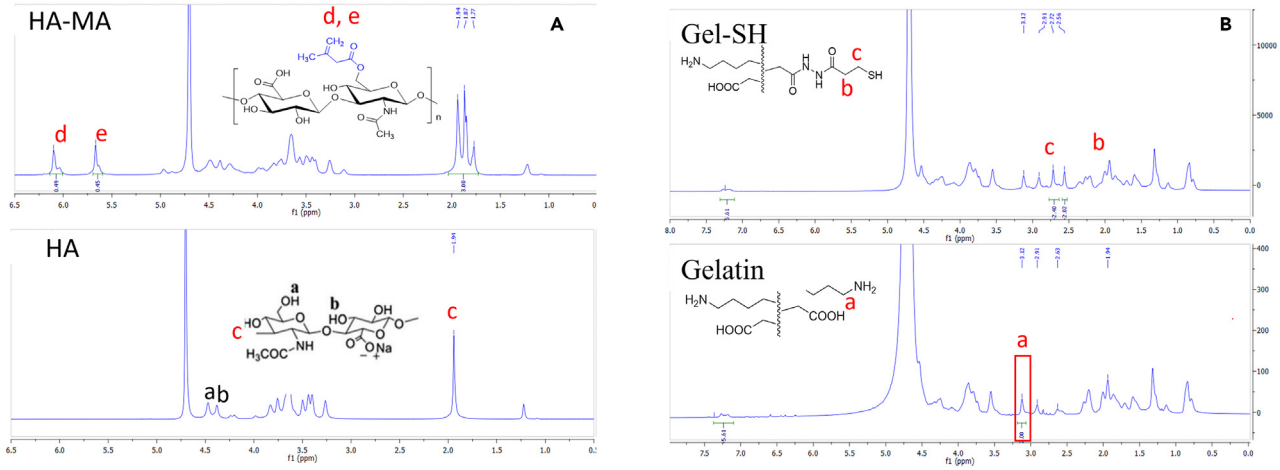

Figure 1. ^{1}H-NMR spectra of the biopolymers

(A) Hyaluronic acid (HA) functionalized to obtain its methacrylated derivative (HA-MA).

(B) ^{1}H-NMR spectra of Gelatin and thiolated gelatin (Gel-SH), showing structural changes in the polymers on functionalization, represented by peaks marked in the ^{1}H-NMR spectra.

(TNB). TNB is a colored species that exhibits a high molar extinction coefficient.[48] The absorbance is measured at 412 nm, and the quantification of results is accomplished using cysteine standard curve. The assay detected 0.81 mmol/g free sulfhydryl groups in the biopolymer Gel-SH (Figure S1).

Physical characterization of Kuragel

The HA-MA and Gel-SH were combined in various combination in the aforementioned range, and the ratio, where HA-MA was 50 mg/mL and Gel-SH was 120 mg/mL ratio, was mixed with the photoinitiator solution and exposed to white light of 10 mW/cm^2 to obtain Kuragel matrix (Figure 2E). These were characterized by extensive physical and chemical methods to demonstrate their suitability for application in healing corneal defects.

Crosslinking kinetics

The crosslinking kinetics study enables an understanding of the reaction rates or the time taken by the pre-polymer solution to transform into a gel, under the influence of light.[49] This process is initiated by the activation of photoinitiators: Eosin Y/TEOA in this case, which absorbs light energy and generates free radicals.[50,51] These reactive species then mediate formation of covalent crosslinks among the methacrylated and thiolated polymers that stabilize the Kuragel structure. The study was performed using a parallel plate rheometer. As shown in Figure 2A, the plot of storage modulus (G′) vs. time revealed the saturation time to be 10 min, beyond which there was no significant increase in the storage modulus on continuous light exposure. This saturation time point was considered as the crosslinking time for the matrix in further experiments. Additionally, no change in G′ was observed in the absence of light, depicting the pre-gel solution did not form gel in 30 min.

Optical characterization

The cornea is a transparent tissue refracting most of the light entering the eye to the lens and retina; the hydrogel to be implanted as a replacement for the cornea tissue must have similar light transmittance properties.[52] In this study, we characterized the visible light (400–700 nm) transmittance of Kuragel. The transmittance curve for the Kuragel in the visible light range is shown in Figure 2B, where the average transmittance was 91.18%, which is similar to that of the human cornea (87%).[1] The transmittance of the Kuragel at all the scan regions was comparable with saline (used as control); a dip observed at 515 nm was due to the presence of Eosin Y with absorbance maxima at 515 nm, in the photoinitiator solution.[53] The photoinitiator gets washed off from the Kuragel improving their transparency overall within a day. The refractive index of the hydrogels was 1.373 which is similar to the native cornea.[54]

Physiochemical characterization

The swelling and degradation of the Kuragel were investigated to understand its structural stability. The hydrogels demonstrated a maximum of 15.28% ± 2.56% and 9.16% ± 2.2% in weight and volumetric swelling, respectively, attained within the first 30 min (Figure 2C).

For successful tissue regeneration, the degradation rate of the hydrogel should align with the regeneration rate of the tissue.[55] A degradation of 6.45% ± 1.53% in PBS and 30.88% ± 2.23% in the presence of enzymes for the Kuragel matrices was observed in a month's time. The cell-encapsulated Kuragels exhibited 9.84% ± 1.73% degradation in media and 42.64% ± 3.94% degradation when cultured in the media

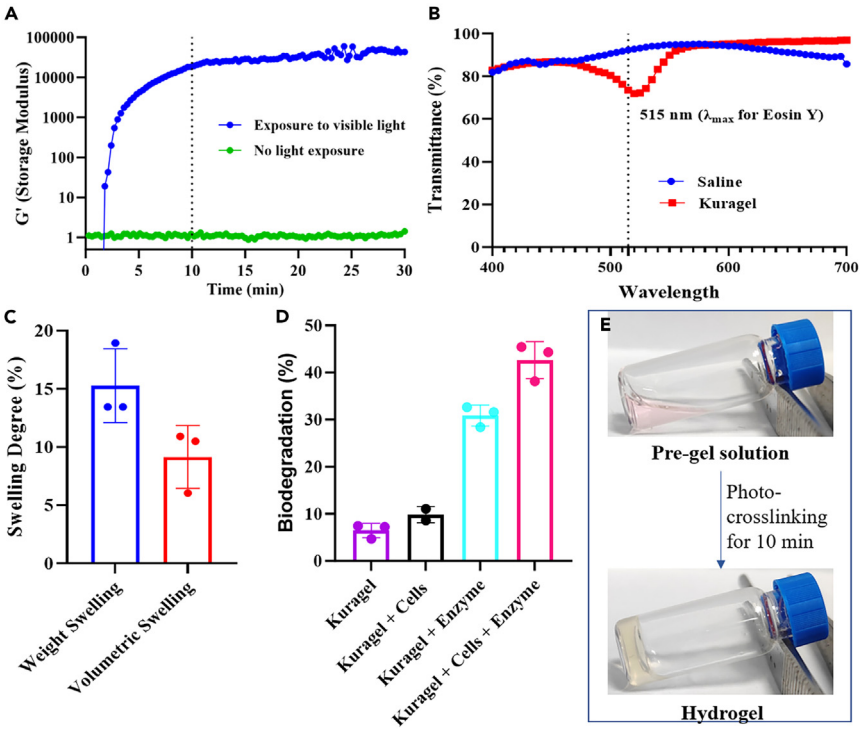

Figure 2. Physiochemical characterization of Kuragel hydrogels

(A) Crosslinking kinetics study of the biopolymer solution on continuous exposure to visible light (10 mW/cm^2), showing saturation of storage modulus after 10 min of exposure. Whereas, the green curve showing no change, depicting no crosslinking or gel formation in the absence of light. Data are representative of curve obtained from n = 3 Kuragel samples.

(B) Transmittance of Kuragel compared to normal saline when measured in the visible light range of 400 nm–700 nm. Data are representative of curve obtained from n = 3 Kuragel samples.

(C) Swelling degree (weight & volumetric) of Kuragel hydrogels. Data are represented as mean ± standard deviation (SD) of n = 3 Kuragel samples.

(D) Biodegradation studies in the presence of enzymes and human corneal stromal cells.

(hCSCs) for a month. Enzyme comprises hyaluronidase (1 U/mL) & collagenase I (0.35 U/mL). Data are represented as mean ± SD of n = 3 Kuragel samples.

(E) Pre-gel solution to hydrogel transition on exposure to visible light for 10 min forming Kuragel.

containing enzymes (Figure 2D). Slow enzymatic degradation would ensure the availability of the matrix support for complete duration of corneal tissue regeneration.[55]

The compressive modulus of the Kuragel was 346.49 ± 18.76 kPa. Matrix stiffness has been reported to modulate the morphology, proliferation, and differentiation state of the cells. The stiffness of Kuragel is similar to that of the native cornea (100–300 kPa) and is expected to promote and support stromal cell survival by providing familiar ECM characteristics.[56]

To ensure the integration of hydrogel with underlying tissue, their adhesion with a biological tissue was determined via adhesion strength analysis. Adhesion of the bioengineered formulation to the surrounding host tissue is essential to prevent premature detaching.[3] The Kuragels demonstrated an adhesion strength of 54.17 ± 6.31 kPa to the porcine skin. The adhesion strength of Kuragel to the corneal tissue is attributed to covalent bond formation between the hydrogel and tissue, arising from the free radicals generated during photo-crosslinking.[57,58] Polymer chains have the capability to bind to biological tissues by establishing covalent bonds with accessible nucleophiles, such as amines, thiols, and hydroxyl groups found on the tissue surfaces,[59,60] as a component of their ECM. The covalent bonds formed between the methacrylate groups in the hydrogel and the thiol groups on the tissue would also contribute to the adhesion of Kuragel hydrogels (Figures S2A and S2C). In addition, hydrogen bonding between the free hydroxyl and amide groups in the polymers also contributes to the adhesion of Kuragel to the host tissue.[27] The presence of these groups in Kuragel was evident in Fourier transform infrared (FTIR) analysis. FTIR spectra of HA-MA and Gel-SH both displayed distinctive amide peaks[61] typically found in biological proteins (Figure S2B). Specifically, the C=O stretching vibration was evident at 1,630 cm^{-1}, while the N-H bending and C-N stretching vibrations were detected at 1,540 and 1,237 cm^{-1}, respectively, in Gel-SH.[61,62] The O-H stretching at 3,370 cm^{-1} in both the polymers further contributes in adhesiveness of Kuragel to the wound site. Furthermore, the methacrylate group in HA-MA as seen via C-O peak at 1,320 cm^{-1} and C=C stretching at 1,636 cm^{-1} ensures adherence of Kuragel to the thiol groups present in the wound surface of cornea.[59,60,63]

The adhesive strength of a commercially available fibrin-based tissue sealant (Tisseel, Baxter, USA) was 105.04 ± 44 kPa. The fibrin-based sealant shows stronger adhesion but has low stability and forms a white layer at the site of administration,[15] which makes its use unsuitable for

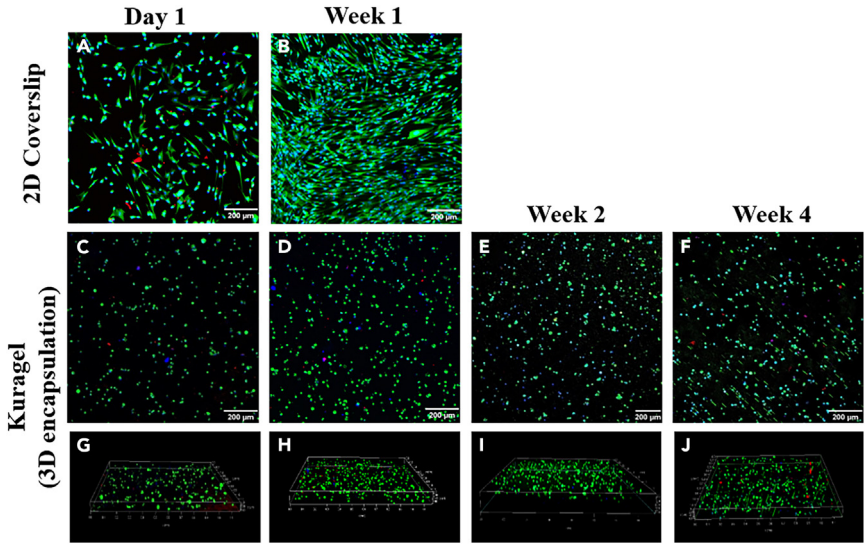

Figure 3. *In vitro* biocompatibility assessment of the hCSCs in the Kuragel hydrogels

The micrographs are representative images obtained from $n = 3$ replicates of Kuragel and 2D coverslips.

(A and B) Live/Dead assay of cells seeded on 2D coverslips.

(C–F) Viability of cells encapsulated in the Kuragel hydrogels showing the progression of viable cell population over 4 weeks.

(G–J) The 3D projection of the frames captured for the hydrogels shows homogeneous viable cell distribution. Viable cells are represented in green, with cell nuclei stained blue and dead cells appearing red. *Scale bar, 200 µm.* See also Table S1.

the application in the cornea that requires transparency for supporting vision restoration. The observations of physiochemical characterization represent that Kuragel has enough strength to support the wounded cornea tissue mechanically and get well integrated with the host tissue, along with showing cornea mimetic properties. This was further assessed by *in vitro* compatibility study with corneal stromal cells followed by validation in a rabbit corneal wound model.

In vitro biocompatibility assessment

The optimal corneal replacement should be biocompatible and non-toxic to the cells in the surrounding tissue. The Kuragel samples were analyzed for cellular viability using calcein AM and ethidium homodimer dyes. The encapsulated human corneal stromal cells (hCSCs) were observed to be viable and homogeneously distributed in Kuragel throughout the study. The viable cell population remained similar in the Kuragel (3D encapsulation) and 2D coverslip on day 1 (approximately 91%) which showed an increase to 94% in 1 week and was maintained over the period of 4 weeks of study (Figures 3C–3J and Table S1). Cells encapsulated in Kuragel appear less elongated than the 2D coverslip cultured cells, owing to the difference in available surface area for the cells to attach and spread, which does not affect their viability.

These results indicate that Kuragel successfully provides a compatible environment for the encapsulated stromal cells. The observations from *in vitro* studies support the fact that the developed Kuragel has well-defined cornea mimetic physical properties and is compatible with stromal cells to integrate with the host tissue. Thus, the study was further extended to assess the efficacy of the hydrogel matrix in a physical injury cornea wound model in New Zealand white rabbits.

In vivo efficacy of Kuragel in New Zealand white rabbits

Corneal clarity evaluation by slit lamp

The ocular surface mechanical injury was evaluated over a period of 3 months to appreciate the changes in cornea clarity, re-epithelialization, neovascularization, and corneal thickness. As the limbus was not damaged, re-epithelization began immediately, accelerating the healing process. The Kuragel-treated group showed corneal clarity and complete re-epithelization within a month, without any scar formation and neovascularization over the period of 90 days (Figures S3 and S4), whereas the wounded untreated group exhibited signs of corneal thinning and scar in the central corneal region on 90th day of observation (Figure 4).

Restoration of corneal thickness and hyperreflectivity

Pachymetry scans provide corneal thickness, and hyperreflectivity is the indication of corneal opacity (higher hyperreflectivity correlates to light obstruction and opaqueness of the cornea); both of these readouts were collected from anterior segment optical coherence tomography (AS-OCT). The pachymetry-based reading for healthy rabbit cornea shows it was 370 $\pm$ 9.4 µm thick. As observed in Figure 5, upon mechanical injury, there was a significant increase in central and peripheral corneal thickness as compared to the healthy cornea, due to underlying inflammation and corneal edema. The average central and peripheral corneal thickness noted in the diseased state was 432 $\pm$ 24 µm

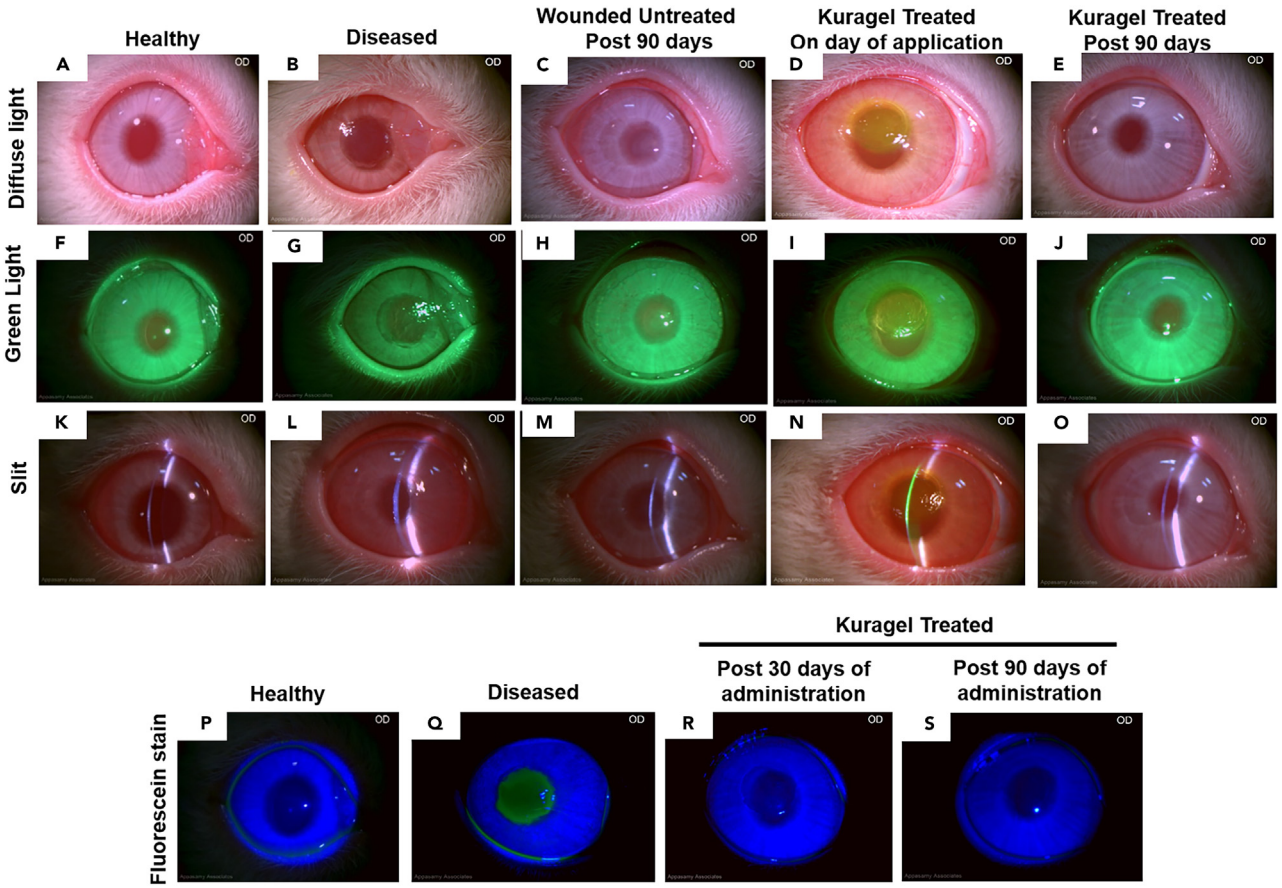

Figure 4. Slit lamp examination of healthy, diseased, wounded untreated, and Kuragel-treated rabbit cornea at the time of administration and post 90 days of treatment

(A–E) Diffuse light indicates cornea clarity.

(F–J) Green light indicates neo-vascularization.

(K–O) Slit beam indicates complete corneal curvature.

(P–S) Fluorescein stain indicates an epithelial defect in the cobalt blue filter. See also Figures S3 and S4.

(central 0–2 mm diameter) and 441 ± 17 μm (peripheral 2–5 mm diameter). Post treatment of the wounded cornea with Kuragel, the corneal thickness was restored to near normal (366 ± 12 μm), unlike untreated where the thickness was significantly reduced (300 ± 13 μm) in 90 days. Kuragel can be seen in the AS-OCT images till day 15 (Figure S5). Post day 15, Kuragel integrates with the native corneal stroma, making it difficult to differentiate by AS-OCT or by H&E staining.

Hyperreflectivity is an indicator of opacity. Opaque cornea generates red signal whereas yellow-green signals represent transparent cornea. As shown in Figure 5C, yellow and green color were observed in healthy state, indicating transparent cornea. In the diseased state (Figure 5E), there was an increase in hyperreflectivity, which was depicted by orange-red color throughout the cornea indicating the presence of opacity in the deep stromal regions close to the endothelium. Though the Kuragel-treated cornea appeared inflamed initially (Figure 5G), the hyperreflectivity was not observed from the day of application till 90 days (Figure 5H). This implied cornea mimetic properties of the Kuragel, making it an ideal corneal ECM substitute. While the untreated arm showed signs of hyperreflectivity and significant thinning in 90 days.

Transparency evaluation by Pentacam

Corneal transparency was assessed by recording the opacity score using Pentacam (Figure 6). An increase in opacity score was observed post trephination injury at the central (0–2 mm diameter) and peripheral (0–6 mm diameter) regions spanning the visual axis (opacity score 38 ± 3.6 for diseased and 25 ± 0.6 for healthy). The wounded untreated cornea showed a significantly high opacity score at the central visual axis 62 ± 6.5 and peripheral 40 ± 2.4 visual axis after 90 days of mechanical injury. Kuragel treatment significantly decreases corneal opacity score (central visual axis opacity score 30 ± 3.2 and peripheral opacity score 32 ± 2.5). The Kuragel treatment restored transparency of the cornea similar to a healthy cornea, while the untreated rabbits showed signs of increased opacity, fibrosis, and thinning.

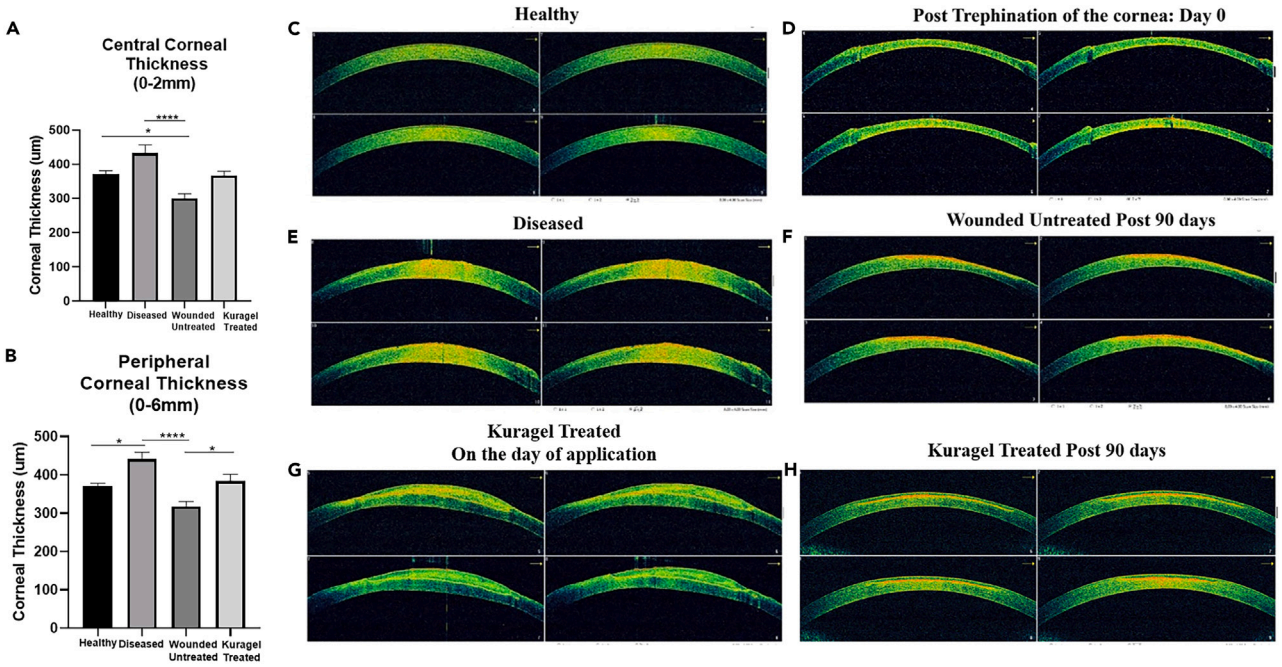

Figure 5. Pachymetry (corneal thickness and hyperreflectivity) of healthy, diseased, wounded untreated, and Kuragel-treated rabbit cornea post 90 days of treatment

(A and B) Central corneal thickness and peripheral corneal thickness of the subsequent groups. Healthy represents a pre-operative state while diseased state represents a day after mechanical injury. Wounded untreated represents creation of mechanical injury model without any treatment. Wounded untreated and Kuragel treated are representative images of the rabbit cornea post 3 months. Bar graphs represent a statistically significant difference in central (0–2 mm) and peripheral (0–6 mm) corneal thickness post 90 days of Kuragel treatment in comparison to other study arms. The * represents statistically significant data (p value ≤ 0.05) between various study arms (* means p value ≤ 0.05, ** ≤ 0.005, *** ≤ 0.0005, and **** ≤ 0.0001).

(C–H) Hyperreflectivity in rabbit cornea for all the 4 groups. Data are represented as mean ± SD. See also Figure S5.

Corneal epithelium, sub-basal nerves, and stromal tissue regeneration evaluation by IVCM

In vivo confocal microscopy (IVCM) was used to evaluate the stratification of corneal epithelium and regeneration of sub-basal nerve fibers and stromal tissue. Since the imaging is performed on live animals, where the objective of the microscope touches the eye, increasing the discomfort when the wound was freshly created, it was not performed for the diseased rabbit group. Among the 3 groups studied by IVCM, a healthy stratified cornea epithelium can be observed in healthy and Kuragel-treated rabbit cornea (Figure 7). Corneal epithelium in the wounded untreated group showed flattened structure and decreased epithelial cell density. Extensive nerve regeneration was observed in the Kuragel-treated rabbit cornea as compared to the untreated group where poor nerve density was seen. Similarly, the regenerated stromal tissue in Kuragel group appeared similar to the healthy rabbit corneal stromal tissue. The wounded untreated group showed irregular stromal layers with hyperreflective keratocytes, an indication of fibrosis. There was no effect of mechanical injury on the endothelial cell layer.

Stratified corneal epithelium with stromal regeneration analysis by histology

The efficacy of Kuragel was evaluated to promote epithelial and stromal regeneration over the period of 90 days using ophthalmological imaging techniques. Post 90 days of treatment, rabbits were euthanized and their eyeballs were evaluated for tissue-level changes among different groups. Stratified corneal epithelium was observed in Kuragel-treated and healthy rabbit tissues, whereas the wounded untreated group showed thicker, irregular, and disoriented corneal epithelium and signs of epithelial hyperplasia (Figures 8A–8D). A near-normal regenerated stroma was also evident in Kuragel-treated rabbits. In the diseased group, where the tissues were obtained from day 1 after injury, excess edema with immune cells infiltration was observed.

A complete corneal recovery can be achieved only when the implant or transplant is capable of reinstating the healthy state. Kuragel treatment on the mechanical injury wound model in rabbit corneas demonstrated reversal of the diseased state and near-healthy state in terms of corneal thickness, transparency, epithelial cell, keratocytes, and nerve density as shown in Figure 8E. The parameters represented in the plot are on a relative scale of 0–10, where the scheme of conversion from original machine readout to relative scoring is provided in the Table S2.

DISCUSSION

Corneal defects, including damage to its structure and shape, are a common cause of blindness and vision impairment. The limitations of corneal grafts are donor-to-donor quality difference leading to lack of consistency, scalability, risk of infection, and the requirement of

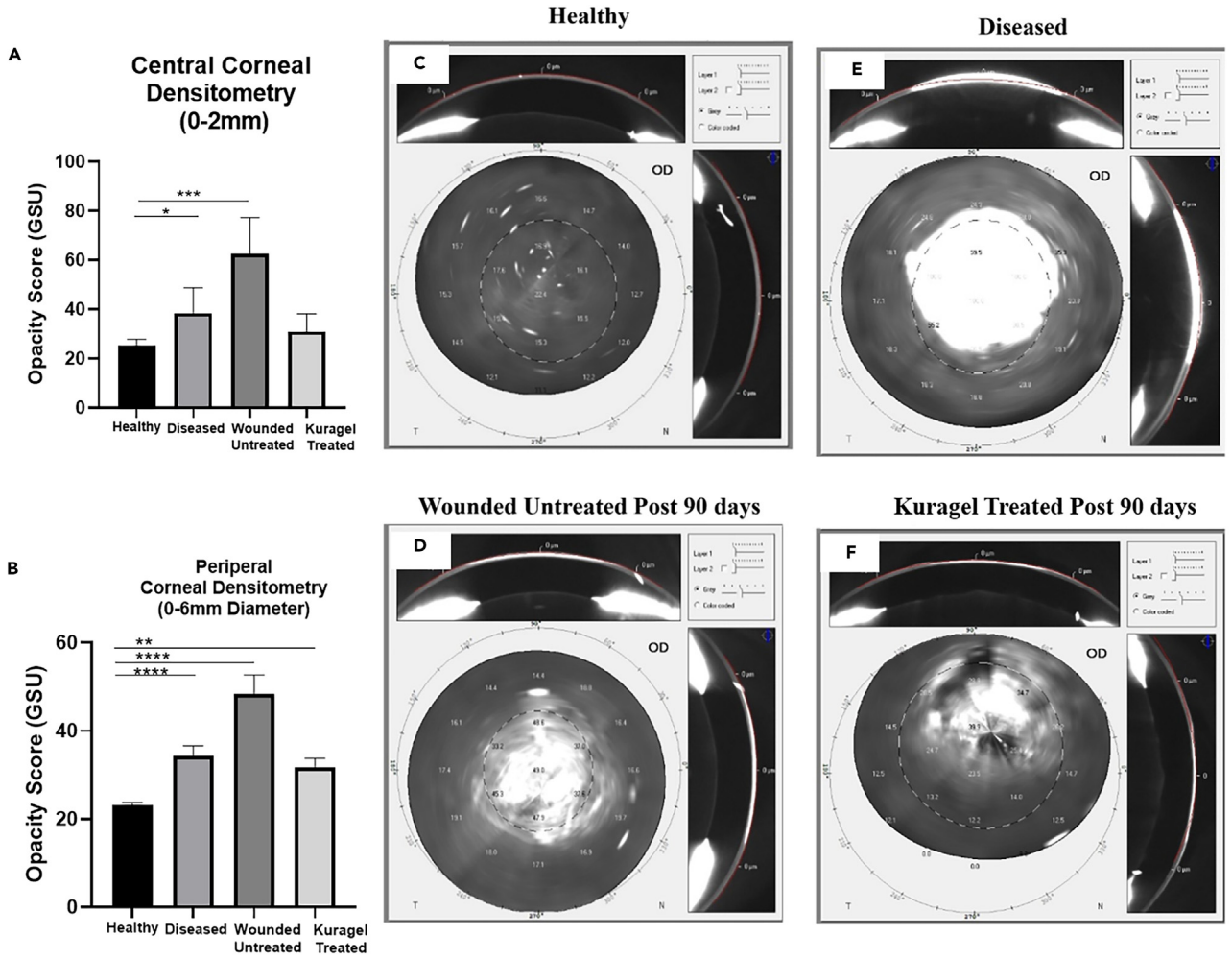

Figure 6. Opacity score (an indicator of transparency) obtained from healthy, diseased, untreated, and Kuragel-treated rabbit corneas obtained through Pentacam

Healthy represents a pre-operative state while diseased state represents a day after mechanical injury. Wounded untreated represents the creation of a mechanical injury model without any treatment. Wounded untreated and Kuragel treated are representative images of the rabbit cornea after 3 months.

(A and B) Bar graphs represent the quantified opacity score in the central visual axis (0–2 mm) post 90 days of Kuragel treatment which appears similar to a healthy cornea opacity sore. Peripheral (0–6 mm) corneal opacity score post 90 days of Kuragel treatment was considerably lower than the untreated group. The * represents statistically significant data (p value ≤ 0.05) between various study arms (* means p value ≤ 0.05, ** ≤ 0.005, *** ≤ 0.0005, and **** ≤ 0.0001).

(C–F) Pentacam images of rabbit cornea obtained post 3 months of administration for all the 4 groups. Data are represented as mean ± SD.

suturing. The conventional standard of care for patients suffering from epithelial and stromal defects also involves tissue adhesives. The standard tissue adhesives, such as cyanoacrylate-based Dermabond, are associated with increased ocular surface inflammation, corneal neovascularization, and giant papillary conjunctivitis, affecting healing and vision.[64] Our work here demonstrates an alternative treatment modality, using a cornea mimetic hydrogel scaffold capable of promoting scarless regeneration of epithelium and stroma. We have developed Kuragel to mimic the physiochemical and biological properties of the native cornea using base polymers of gelatin and HA, which are generally regarded as safe (GRAS), functionalized via thiolation and methacrylation, respectively.[65–67] Previous studies report HA may help in facilitating the migration of corneal epithelial cells and promoting wound repair.[68] CD44, a receptor known to interact with HA, possesses an extracellular HA-binding domain and an intracellular domain capable of interfacing with cytoskeletal proteins and modulating cell signaling, cell migration, and cell proliferation.[6,69] Furthermore, the therapeutic potential of topical HA has been substantiated *in vivo*.[6] Gelatin is one of the most extensively used biopolymer for cell-based and *in vivo* studies.[3] We adopted visible light-based crosslinking mechanism, which has recently gained popularity for matrix preparation for application in tissue engineering-based approaches. Previously, human mesenchymal stem cells (hMSC)-laden hydrogels of thiolated HA and poly(butynyl phospholane)-random-poly(ethylethylene phosphate) were fabricated using ultraviolet light crosslinking (365 nm), which exhibited favorable biocompatibility.[70] Another study demonstrated preparation of a biocompatible and transparent bioadhesive for corneal reconstruction using visible light crosslinking of methacrylated gelatin. They showed fine-tuning of

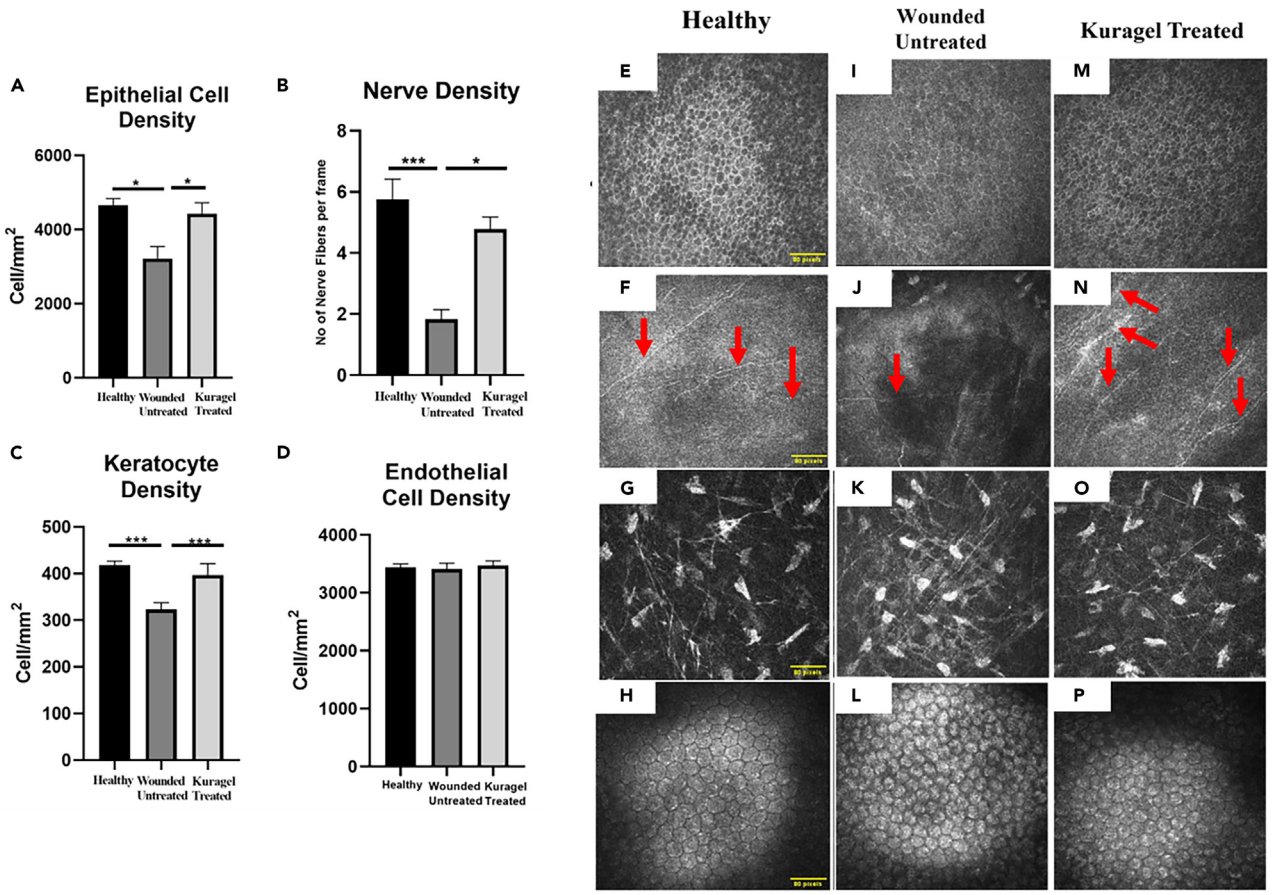

Figure 7. Cell density evaluation of different cornea layers by *in vivo* confocal microscopy (IVCM) to demonstrate effect of Kuragel in reversal of epithelium and stromal injury

Healthy represents the pre-operative state while wounded untreated depicts the creation of mechanical injury model without any treatment.

(A–C) Bar graphs representing statistically significant difference in epithelial cell, nerve fiber, and keratocyte density post 90 days of Kuragel treatment in comparison to other study arms.

(D) Endothelial cell density remains unaffected in the diseased animal post trephination-,based mechanical injury to epithelium and stroma as well as post Kuragel administration. * represents statistically significant data (p value $\leq$ 0.05) between various study arms (* means p value $\leq$ 0.05, **$\leq$0.005, ***$\leq$ 0.0005, and ****$\leq$0.0001). Data are represented as mean $\pm$ SD.

(E–H) IVCM images of healthy unwounded rabbit cornea.

(I–L) IVCM images of wounded untreated cornea.

(M–P) IVCM images after application of Kuragel on the wounded cornea post 3 months. Scale bars in micrographs E to P represent 80 pixels, where 1 pixel = 0.8 μm.

the physical properties of the hydrogel by changing polymer concentration and photo-crosslinking time.[3] We optimized the biopolymeric Kuragel formulation by screening different concentration ratios of the biopolymers HA-MA and Gel-SH. The target properties were set based on the properties of native cornea stroma reported in literature, like 300 kPa compressive modulus,[56] 87% transmittance to visible light,[1] low swelling (desired range was <20%), and high adhesive strength[3] (desired values higher than 40 kPa). The HA-MA was used between 40 and 80 mg/mL, and the concentration of Gel-SH was varied between 50 and 140 mg/mL. The hydrogels prepared using biopolymers lower than the optimized ratio of 50 mg/mL HA-MA and 120 mg/mL Gel-SH did not form a stable gel in 10–12 min of light exposure, and the weak hydrogels thus formed showed more than 40% swelling. Whereas, increase in their concentration resulted in stiffer hydrogels where their modulus was above 500 kPa. As the physical properties of the hydrogels from other ratio were very distant from meeting the requirements for a substitute for cornea tissue, the data for the same are not included in the manuscript and were not considered for biological characterization.

Hydrogels have innate tendency to swell when exposed to physiological fluid. Modulating the swelling degree of hydrogels is regarded as a key aspect of regenerative medicine, especially in corneal regeneration. A high swelling hydrogel can lead to complications like increased intraocular pressure and corneal distortion followed by inflammation and tissue damage.[71] The composition of Kuragel containing HA-MA and Gel-SH was carefully optimized to restrict swelling to less than 20% (in terms of weight as well as volume).[72] To fill irregular defect sites effectively, it is desirable for Kuragel formulation to have a lower swelling tendency to prevent bulging in the later stages.[73] Additionally, in the case of the cornea, it is expected that Kuragel will maintain its thickness to prevent the development of conditions similar to astigmatism.[73]

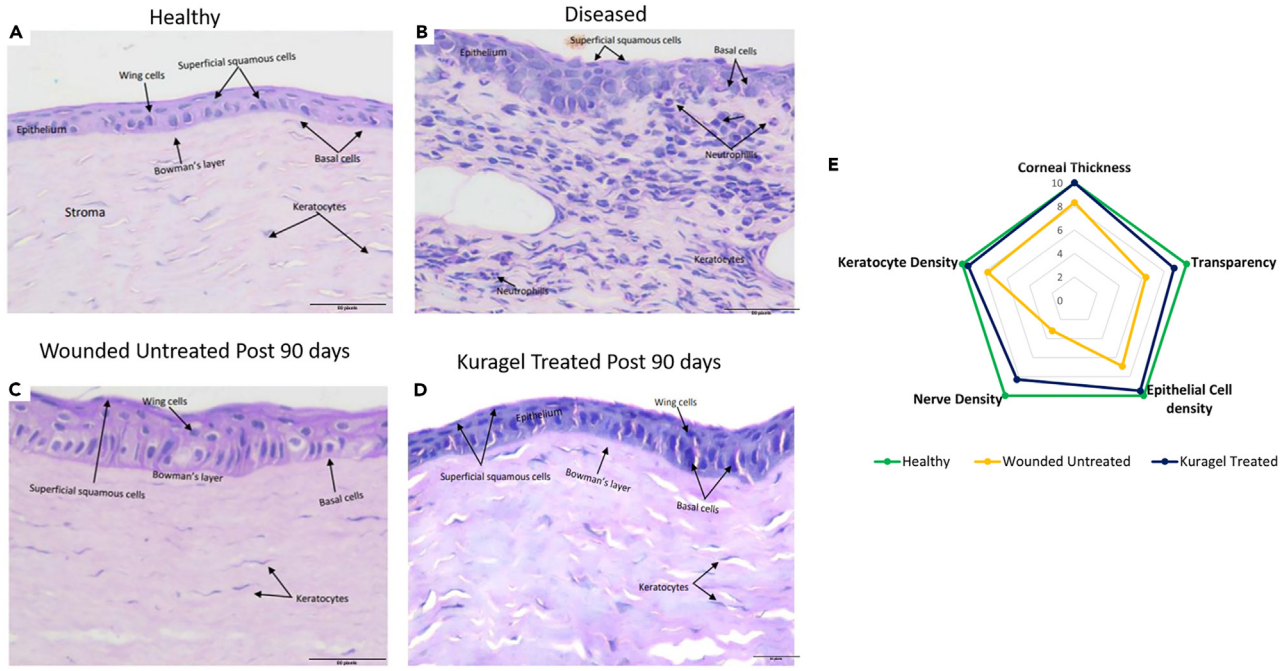

Figure 8. Histological analysis and representation of data from Kuragel-treated rabbit cornea post administration

(A–D) H&E staining of the cornea from different study arms. Healthy represents pre-operative state while diseased state represents a day after mechanical injury. Wounded untreated represents creation of a mechanical injury model without any treatment. Wounded untreated and Kuragel treated are representative images of the rabbit cornea after 3 months. Scale bar 80 pixels; 1 pixel = 0.264 mm.

(E) Radar plot representation of corneal tissue states derived from pachymetry, densitometry, and IVCM data obtained from healthy rabbits, as well as rabbits treated with and without Kuragel (after 90 days of trephination induced injury). Corneal thickness, transparency, epithelial cell, nerve, and keratocyte density are represented here on a relative scale of 0–10, showing a near-healthy state of Kuragel treatment. See also Table S2.

Further, the compressive modulus of Kuragel is 350 kPa which matches the modulus of human cornea.[3] Prior study on poly(ε-caprolactone)-poly(ethylene glycol) microfibrous scaffold infused with Gel-MA hydrogel generated a 3D fiber hydrogel construct.[72] However, those hydrogels were soft and had less resident time at the site. Another important characteristic that is instrumental in defining the success of corneal hydrogels is the light transmittance post-application. Since the cornea is transparent, it is paramount that the hydrogels intended for corneal regeneration should be transparent. The Kuragel matrix is 91% transparent, which meets the requirement of the transparency of native cornea i.e., a minimum of 87%. Bioengineered porcine collagen hydrogels have also been reported to mimic the properties of native corneal tissue and have recorded an optical transmittance of 90% in the visible wavelength range.[7] Gentamicin-loaded methacrylate-silk hydrogels were also investigated for corneal regeneration and recorded an optical transmittance of 80%–83%.[74]

Kuragel was prepared for administration in the wounded cornea and expected to regenerate the damaged cornea. Adhesion with the host tissue would ensure the Kuragel matrix remains at the site of injury throughout the treatment, and a gradual degradation would support the regeneration of the host tissue. Kuragel showed an adhesion strength of 54.17 $\pm$ 6.31 kPa. This adhesion is far superior than many other corneal substitutes reported in the literature and will ensure the well-integrated hydrogels at the corneal site. It is higher than the reported values of clinically available sealants which are PEG based, CoSEAL (Baxter, USA) with strength of 19.4 $\pm$ 17.3 kPa, and fibrin-based Evicel (Ethicon, USA) having adhesion strength of 26.3 $\pm$ 4.7 kPa).[3] The observed adhesion strength is lower as compared to that of a gelatin-based sealant 90.4 $\pm$ 10.2 kPa.[3] Though these gels show higher adhesion, they get degraded completely within a month, making their use unsuitable for deep or larger wounds that require support for prolonged duration. The most recent findings where decellularized porcine cornea extracellular matrix (LC-COMatrix) containing un-denatured collagen and sulfated glycosaminoglycans was used to secure corneal defects reported an adhesive strength of 21.8 $\pm$ 2.3 kPa.[65] Further, we performed *in vitro* biodegradation study in the presence of hyaluronidase and collagenase enzymes. The Kuragel matrix degraded minimally in the absence of enzymes; however, the degradation was enhanced in the presence of enzymes and cells. The degradation rates are in line with the degradation rates of native human cornea in the presence of collagenase enzyme. A study reported that the native human corneal tissue when exposed to collagenase for 10 days recorded a weight reduction by 68.8% $\pm$ 5.3%.[65] The Kuragels degraded by 42.64% $\pm$ 3.94% in the presence of enzymes and encapsulated hCSCs, which confirms that the Kuragel matrix would be able to withstand the ocular environment and is expected to support controlled healing.

Corneal implants should be biocompatible and non-toxic to the native cells. The viability assessment demonstrated that the Kuragel composition and processing steps are not posing any harm to cell viability. It also ensured that the hydrogel matrix allows the nutrients from media to be available to encapsulated cells to maintain their viability. The *in vitro* observations demonstrate that the Kuragel has

well-defined cornea mimetic physical properties and are compatible with corneal stromal cells. They are similar to native corneal ECM in chemical makeup, as HA and gelatin (hydrolyzed collagen) are abundantly found in corneal stromal region, and are known to support the cell phenotype.[75] Such corneal implants can aid in providing required regenerative cues.

The standard management protocol for corneal stromal defects has significant shortcomings, including poor biomechanical, optical, or adhesive properties, as well as a lack of suitable cornea for transplant, or rejection leading to poor outcomes. To address these limitations, in this study, we developed a biocompatible smart gel, Kuragel which can be applied dropwise at the wound site. Our results show that the Kuragel provides not only a native cornea-like structure but also the topography and smooth contour. In line with the *in vitro* data, *in vivo* study shows that Kuragel effectively polymerizes within 10 min under white light, bypassing the need for sutures. Other groups have also aimed to develop tissue-engineered transplants for the treatment of corneal epithelial defects and stromal ulcers to reduce the need for corneal tissue. However, the majority of these methods are based on prefabricated membranes[76] or patches,[77] which typically require surgical equipment and skills. Kuragel also promoted faster epithelialization and stromal regeneration compared to the untreated group.

Studies conducted in the past to evaluate the efficacy of biopolymeric implants in regenerating cornea used either slit lamp or AS-OCT to evaluate corneal regeneration. One of the critical considerations to take into account while studying corneal reconstruction is the way the cornea is evaluated to make it clinically successful. In the present study in New Zealand white rabbits with corneal wounds, we implemented more comprehensive set of clinical imaging parameters used in the clinical setup for the patients, including slit lamp, AS-OCT, Pentacam, and IVCM. It was evident that Kuragel treatment not only restored the thickness of the cornea like healthy rabbit cornea, but it also improved the corneal transparency (opacity score) and clarity by significantly reducing the scarring (decreased hyperreflectivity). On the other hand, mechanical injury with no Kuragel treatment resulted in significant corneal thinning with scarring as evident from the AS-OCT pachymetry and Pentacam studies. The observations from IVCM showing improved epithelium and nerve regeneration further strengthen our findings. Kuragel treatment resulted in stratified corneal epithelium similar to a healthy cornea, with regeneration of sub-basal nerve fibers, whereas the non-treated rabbits showed poor stratification, with hyperplasia as evident from H&E images. Sub-basal nerve fibers were also significantly fewer in the untreated group compared to the healthy and Kuragel-treated groups. IVCM and histology collectively showed that Kuragel treatment resulted in keratocyte proliferation and restoration of corneal stromal mass over the period of 90 days, whereas the untreated rabbits' thinner cornea with hyper-reflective keratocytes was observed as an indication of fibrosis and lack of regeneration.

In conclusion, if engineered substitutes for human donor corneal tissue are not developed for keratoplasty, there will continue to be a lack of resources for treating large-scale corneal wounds in patients. While there have been notable improvements in creating cell-based materials that closely resemble the cornea's layers, these advancements have not yet resulted in the introduction of new cell-infused or cell-free natural biopolymer implants to the market. The utilization of sutures in keratoplasty is a time-consuming process along with bringing about numerous complications during the postoperative phase. To address this concern, we have formulated a photo-crosslinkable bioadhesive hydrogel, comprising HA-MA and Gel-SH, as an alternative to traditional sutures in keratoplasty. Our scalable tissue-engineered corneal implant embodies the characteristics desirable for effective corneal adhesion, encompassing remarkable light transmittance, optimal swelling, resistance against enzymatic degradation, suitable matrix stiffness, and good biocompatibility. The investigations have indicated that the hydrogel supports growth of epithelial cells on the upper layer and stromal cells in the inner mass. These findings have been consistently substantiated by experiments conducted on New Zealand white rabbits. In these trials, a mechanical wound spanning the central visual axis of the stroma exhibited complete closure upon treatment with the hydrogels. The recuperation process was characterized by full re-epithelialization within 1 month, as observed through slit lamp examination. Additionally, within 3 months, there was evidence of keratocyte repopulation, and IVCM displayed regeneration of the sub-basal nerve plexus near healthy tissue. Densitometry and pachymetry evaluations unveiled the restoration of corneal clarity, optical density, and thickness, comparable to those of a healthy cornea, within 2 months following the application of the hydrogel. This helps in restoring the cornea in its healthy state with transparency and corneal thickness via epithelium, stroma, and neuronal regeneration, making it applicable for diverse corneal indications including corneal thinning. The methodology adapted here to develop cornea-specific problems is based on first principle of quality-by-design. Its potential use includes a minimally invasive treatment for diseases such as advanced keratoconus via intra-stromal pocket generation using laser and injecting Kuragel. The production and application approaches adapted for the Kuragel can also be applied in other tissues based on the tissue- and disease-specific needs.

Limitations of the study

This study illustrates the cornea mimetic nature of Kuragel covering key *in vitro* properties and demonstrating their translation *in vivo* in a rabbit wound model. The Kuragel, besides filling the corneal wounds, also showed remarkable healing properties, which can be potentially enhanced by their use as delivery vehicle for cell modulators, extracellular vesicles, and stem cells,[78] though not explored in this study. The use of Kuragel, in the current study, is limited to regeneration of cornea primarily based on re-epithelization and stromal thickness restoration; however, it can be extended further for deeper wounds with endothelium damage.

STAR★METHODS

Detailed methods are provided in the online version of this paper and include the following:

- KEY RESOURCES TABLE
- RESOURCE AVAILABILITY
  - Lead contact

SUPPLEMENTAL INFORMATION

Supplemental information can be found online at https://doi.org/10.1016/j.isci.2024.109641.

ACKNOWLEDGMENTS

The authors acknowledge Bangalore Bioinnovation Centre, India for providing resources for carrying out *in vitro* studies. The authors thank Mission Bay Capital, MBC Biolabs, San Francisco, USA for supporting the research. The authors also extend their thanks to Dabur Research Foundation, India for providing infrastructure for carrying out studies in rabbits.

AUTHOR CONTRIBUTIONS

Conceptualization, T.B. and A.C.; methodology and validation, P.A., A.T., A.G., A.V.K., and R.H.; investigation, P.A., A.G., S.K.C., M.V., N.W., U.B., K.S., B.S., J.R., R.R., and N.P.R.; project administration, P.A. and A.T.; writing – original draft, P.A., A.T., and M.V. with inputs from all the authors; writing – review and editing, P.A., S.K.C., A.T., and T.B.; resources, T.B., A.C., and V.S.S.; supervision, T.B., V.S.S., R.H., and A.V.K.

DECLARATION OF INTERESTS

We declare the patent application, WO2023209738A1, filed by Pandorum Technologies Pvt. Ltd., comprises information related to this work where T.B., P.A., S.K.C., and K.S. are inventors.

Received: September 7, 2023
Revised: January 30, 2024
Accepted: March 26, 2024
Published: March 28, 2024

REFERENCES

1. Islam, M.M., Buznyk, O., Reddy, J.C., Pasyechnikova, N., Alarcon, E.I., Hayes, S., Lewis, P., Fagerholm, P., He, C., Iakymenko, S., et al. (2018). Biomaterials-enabled cornea regeneration in patients at high risk for rejection of donor tissue transplantation. NPJ Regen. Med. *3*, 2. https://doi.org/10.1038/s41536-017-0038-8.
2. Deshmukh, R., Stevenson, L.J., and Vajpayee, R. (2020). Management of corneal perforations: An update. Indian J. Ophthalmol. *68*, 7–14. https://doi.org/10.4103/ijo.IJO_1151_19.
3. Shirzaei Sani, E., Kheirkhah, A., Rana, D., Sun, Z., Foulsham, W., Sheikhi, A., Khademhosseini, A., Dana, R., and Annabi, N. (2019). Sutureless repair of corneal injuries using naturally derived bioadhesive hydrogels. Sci. Adv. *5*, eaav1281. https://doi.org/10.1126/sciadv.aav1281.
4. Zhu, M., Wang, Y., Ferracci, G., Zheng, J., Cho, N.-J., and Lee, B.H. (2019). Gelatin methacryloyl and its hydrogels with an exceptional degree of controllability and batch-to-batch consistency. Sci. Rep. *9*, 6863. https://doi.org/10.1038/s41598-019-42186-x.
5. Kilic Bektas, C., and Hasirci, V. (2018). Mimicking corneal stroma using keratocyte loaded photopolymerizable methacrylated gelatin hydrogels. J. Tissue Eng. Regen. Med. *12*, e1899–e1910. https://doi.org/10.1002/term.2621.
6. Chen, F., Le, P., Fernandes-Cunha, G.M., Heilshorn, S.C., and Myung, D. (2020). Bio-orthogonally crosslinked hyaluronate-collagen hydrogel for suture-free corneal defect repair. Biomaterials *255*, 120176. https://doi.org/10.1016/j.biomaterials.2020.120176.
7. Xeroudaki, M., Thangavelu, M., Lennikov, A., Ratnayake, A., Bisevac, J., Petrovski, G., Fagerholm, P., Rafat, M., and Lagali, N. (2020). A porous collagen-based hydrogel and implantation method for corneal stromal regeneration and sustained local drug delivery. Sci. Rep. *10*, 16936. https://doi.org/10.1038/s41598-020-73730-9.
8. Zamboulis, A., Nanaki, S., Michailidou, G., Koumentakou, I., Lazaridou, M., Ainali, N.M., Xanthopoulou, E., and Bikiaris, D.N. (2020). Chitosan and its Derivatives for Ocular Delivery Formulations: Recent Advances and Developments. Polymers *12*, 1519. https://doi.org/10.3390/polym12071519.
9. Tsai, C.-Y., Woung, L.-C., Yen, J.-C., Tseng, P.-C., Chiou, S.-H., Sung, Y.-J., Liu, K.-T., and Cheng, Y.-H. (2016). Thermosensitive chitosan-based hydrogels for sustained release of ferulic acid on corneal wound healing. Carbohydr. Polym. *135*, 308–315. https://doi.org/10.1016/j.carbpol.2015.08.098.
10. Lee, Y.-P., Liu, H.-Y., Lin, P.-C., Lee, Y.-H., Yu, L.-R., Hsieh, C.-C., Shih, P.-J., Shih, W.-P., Wang, I.-J., Yen, J.-Y., and Dai, C.-A. (2019). Facile fabrication of superporous and biocompatible hydrogel scaffolds for artificial corneal periphery. Colloids Surf. B Biointerfaces *175*, 26–35. https://doi.org/10.1016/j.colsurfb.2018.11.013.
11. He, B., Wang, J., Xie, M., Xu, M., Zhang, Y., Hao, H., Xing, X., Lu, W., Han, Q., and Liu, W. (2022). 3D printed biomimetic epithelium/stroma bilayer hydrogel implant for corneal regeneration. Bioact. Mater. *17*, 234–247. https://doi.org/10.1016/j.bioactmat.2022.01.034.

12. Williams, D.L., Wirostko, B.M., Gum, G., and Mann, B.K. (2017). Topical Cross-Linked HA-Based Hydrogel Accelerates Closure of Corneal Epithelial Defects and Repair of Stromal Ulceration in Companion Animals. Invest. Ophthalmol. Vis. Sci. *58*, 4616–4622. https://doi.org/10.1167/iovs.16-20848.
13. Koivusalo, L., Kauppila, M., Samanta, S., Parihar, V.S., Ilmarinen, T., Miettinen, S., Oommen, O.P., and Skottman, H. (2019). Tissue adhesive hyaluronic acid hydrogels for sutureless stem cell delivery and regeneration of corneal epithelium and stroma. Biomaterials *225*, 119516. https://doi.org/10.1016/j.biomaterials.2019.119516.
14. Khosravimelal, S., Mobaraki, M., Eftekhari, S., Ahearne, M., Seifalian, A.M., and Gholipourmalekabadi, M. (2021). Hydrogels as Emerging Materials for Cornea Wound Healing. Small *17*, 2006335. https://doi.org/10.1002/smll.202006335.
15. Chandru, A., Agrawal, P., Ojha, S.K., Selvakumar, K., Shiva, V.K., Gharat, T., Selvam, S., Thomas, M.B., Damala, M., Prasad, D., et al. (2021). Human cadaveric donor cornea derived extra cellular matrix microparticles for minimally invasive healing/regeneration of corneal wounds. Biomolecules *11*, 532. https://doi.org/10.3390/biom11040532.
16. Jangamreddy, J.R., Haagdorens, M.K.C., Mirazul Islam, M., Lewis, P., Samanta, A., Fagerholm, P., Liszka, A., Ljunggren, M.K., Buznyk, O., Alarcon, E.I., et al. (2018). Short peptide analogs as alternatives to collagen in pro-regenerative corneal implants. Acta Biomater. *69*, 120–130. https://doi.org/10.1016/j.actbio.2018.01.011.
17. McTiernan, C.D., Simpson, F.C., Haagdorens, M., Samarawickrama, C., Hunter, D., Buznyk, O., Fagerholm, P., Ljunggren, M.K., Lewis, P., Pintelon, I., et al. (2020). LiQD Cornea: Pro-regeneration collagen mimetics as patches and alternatives to corneal transplantation. Sci. Adv. *6*, eaba2187. https://doi.org/10.1126/sciadv.aba2187.
18. Logan, C.M., Fernandes-Cunha, G.M., Chen, F., Le, P., Mundy, D., Na, K.S., and Myung, D. (2023). In Situ-forming Collagen Hydrogels Crosslinked by Multifunctional Polyethylene Glycol as a Matrix Therapy for Corneal Defects: 2-Month Follow-up In Vivo. Cornea *42*, 97–104. https://doi.org/10.1097/ICO.0000000000003104.
19. Na, K.-S., Fernandes-Cunha, G.M., Varela, I.B., Lee, H.J., Seo, Y.A., and Myung, D. (2021). Effect of mesenchymal stromal cells encapsulated within polyethylene glycol-collagen hydrogels formed in situ on alkali-burned corneas in an ex vivo organ culture model. Cytotherapy *23*, 500–509. https://doi.org/10.1016/j.jcyt.2021.02.001.
20. Arboleda, A., Cunha, G.M.F., Manche, A., Seo, Y.A., Logan, C., Heilshorn, S.C., and Myung, D. (2022). Biocompatibility of photoactivated collagen-riboflavin hydrogels for corneal regeneration. Invest. Ophthalmol. Vis. Sci. *63*, 101–A0199. https://iovs.arvojournals.org/article.aspx?articleid=2779234.
21. Rose, J.B., Pacelli, S., Haj, A.J.E., Dua, H.S., Hopkinson, A., White, L.J., and Rose, F.R.A.J. (2014). Gelatin-Based Materials in Ocular Tissue Engineering. Materials *7*, 3106–3135. https://doi.org/10.3390/ma7043106.
22. Sharifi, S., Islam, M.M., Sharifi, H., Islam, R., Koza, D., Reyes-Ortega, F., Alba-Molina, D., Nilsson, P.H., Dohlman, C.H., Mollnes, T.E., et al. (2021). Tuning gelatin-based hydrogel towards bioadhesive ocular tissue engineering applications. Bioact. Mater. *6*, 3947–3961. https://doi.org/10.1016/j.bioactmat.2021.03.042.
23. Lai, J.-Y., Li, Y.T., Cho, C.H., and Yu, T.C. (2012). Nanoscale modification of porous gelatin scaffolds with chondroitin sulfate for corneal stromal tissue engineering. Int. J. Nanomed. *7*, 1101–1114. https://doi.org/10.2147/IJN.S28753.
24. Jumelle, C., Sani, E.S., Taketani, Y., Yung, A., Gantin, F., Chauhan, S.K., Annabi, N., and Dana, R. (2021). Growth factor-eluting hydrogels for management of corneal defects. Mater. Sci. Eng. C Mater. Biol. Appl. *120*, 111790. https://doi.org/10.1016/j.msec.2020.111790.
25. Barroso, I.A., Man, K., Robinson, T.E., Cox, S.C., and Ghag, A.K. (2022). Photocurable GelMA Adhesives for Corneal Perforations. Bioengineering *9*, 53. https://doi.org/10.3390/bioengineering9020053.
26. Van Hoorick, J., Dobos, A., Markovic, M., Gheysens, T., Van Damme, L., Gruber, P., Tytgat, L., Van Erps, J., Thienpont, H., Dubruel, P., et al. (2020). Thiol-norbornene gelatin hydrogels: influence of thiolated crosslinker on network properties and high definition 3D printing. Biofabrication *13*, 015017. https://doi.org/10.1088/1758-5090/abc95f.
27. Rajabi, N., Kharaziha, M., Emadi, R., Zarrabi, A., Mokhtari, H., and Salehi, S. (2020). An adhesive and injectable nanocomposite hydrogel of thiolated gelatin/gelatin methacrylate/Laponite® as a potential surgical sealant. J. Colloid Interface Sci. *564*, 155–169. https://doi.org/10.1016/j.jcis.2019.12.048.
28. Lee, M., Rizzo, R., Surman, F., and Zenobi-Wong, M. (2020). Guiding Lights: Tissue Bioprinting Using Photoactivated Materials. Chem. Rev. *120*, 10950–11027. https://doi.org/10.1021/acs.chemrev.0c00077.
29. Xu, Q., Torres, J.E., Hakim, M., Babiak, P.M., Pal, P., Battistoni, C.M., Nguyen, M., Panitch, A., Solorio, L., and Liu, J.C. (2021). Collagen- and hyaluronic acid-based hydrogels and their biomedical applications. Mater. Sci. Eng. R Rep. *146*, 100641. https://doi.org/10.1016/j.mser.2021.100641.
30. Dovedytis, M., Liu, Z.J., and Bartlett, S. (2020). Hyaluronic acid and its biomedical applications: A review. Eng. Regen. *1*, 102–113. https://doi.org/10.1016/j.engreg.2020.10.001.
31. Kim, D.J., Jung, M.-Y., Pak, H.-J., Park, J.-H., Kim, M., Chuck, R.S., and Park, C.Y. (2021). Development of a novel hyaluronic acid membrane for the treatment of ocular surface diseases. Sci. Rep. *11*, 2351. https://doi.org/10.1038/s41598-021-81983-1.
32. Fernandes-Cunha, G.M., Jeong, S.H., Logan, C.M., Le, P., Mundy, D., Chen, F., Chen, K.M., Kim, M., Lee, G.-H., Na, K.-S., et al. (2022). Supramolecular host-guest hyaluronic acid hydrogels enhance corneal wound healing through dynamic spatiotemporal effects. Ocul. Surf. *23*, 148–161. https://doi.org/10.1016/j.jtos.2021.09.002.
33. Chen, F., Le, P., Lai, K., Fernandes-Cunha, G.M., and Myung, D. (2020). Simultaneous Interpenetrating Polymer Network of Collagen and Hyaluronic Acid as an *In Situ* -Forming Corneal Defect Filler. Chem. Mater. *32*, 5208–5216. https://doi.org/10.1021/acs.chemmater.0c01307.
34. Shen, X., Li, S., Zhao, X., Han, J., Chen, J., Rao, Z., Zhang, K., Quan, D., Yuan, J., and Bai, Y. (2023). Dual-crosslinked regenerative hydrogel for sutureless long-term repair of corneal defect. Bioact. Mater. *20*, 434–448. https://doi.org/10.1016/j.bioactmat.2022.06.006.
35. Park, S.K., Ha, M., Kim, E.J., Seo, Y.A., Lee, H.J., Myung, D., Kim, H.-S., and Na, K.-S. (2022). Hyaluronic acid hydrogels crosslinked via blue light-induced thiol-ene reaction for the treatment of rat corneal alkali burn. Regen. Ther. *20*, 51–60. https://doi.org/10.1016/j.reth.2022.03.005.
36. Wang, A., Dong, L., Guo, Z., Sun, W., and Mi, S. (2022). A methacrylated hyaluronic acid network reinforced Pluronic F-127 gel for treatment of bacterial keratitis. Biomed. Mater. *17*, 045017. https://doi.org/10.1088/1748-605X/ac6ea9.
37. Sorkin, N., and Varssano, D. (2014). Corneal Collagen Crosslinking: A Systematic Review. Ophthalmologica *232*, 10–27. https://doi.org/10.1159/000357979.
38. Van Hoorick, J., Tytgat, L., Dobos, A., Ottevaere, H., Van Erps, J., Thienpont, H., Ovsianikov, A., Dubruel, P., and Van Vlierberghe, S. (2019). Photo-)crosslinkable gelatin derivatives for biofabrication applications. Acta Biomater. *97*, 46–73. https://doi.org/10.1016/j.actbio.2019.07.035.
39. GhavamiNejad, A., Ashammakhi, N., Wu, X.Y., and Khademhosseini, A. (2020). Crosslinking Strategies for 3D Bioprinting of Polymeric Hydrogels. Small *16*, 2002931. https://doi.org/10.1002/smll.202002931.
40. Chalard, A.E., Dixon, A.W., Taberner, A.J., and Malmström, J. (2022). Visible-Light Stiffness Patterning of GelMA Hydrogels Towards In Vitro Scar Tissue Models. Front. Cell Dev. Biol. *10*, 946754. https://doi.org/10.3389/fcell.2022.946754.
41. Sani, E.S., Lara, R.P., Aldawood, Z., Bassir, S.H., Nguyen, D., Kantarci, A., Intini, G., and Annabi, N. (2019). An Antimicrobial Dental Light Curable Bioadhesive Hydrogel for Treatment of Peri-Implant Diseases. Matter *1*, 926–944. https://doi.org/10.1016/j.matt.2019.07.019.
42. Sharifi, S., Sharifi, H., Akbari, A., and Chodosh, J. (2021). Systematic optimization of visible light-induced crosslinking conditions of gelatin methacryloyl (GelMA). Sci. Rep. *11*, 23276. https://doi.org/10.1038/s41598-021-02830-x.
43. Zhang, F., and King, M.W. (2020). Biodegradable Polymers as the Pivotal Player in the Design of Tissue Engineering Scaffolds. Adv. Healthc. Mater. *9*, 1901358. https://doi.org/10.1002/adhm.201901358.
44. Martin, I., Simmons, P.J., and Williams, D.F. (2014). Manufacturing Challenges in Regenerative Medicine. Sci. Transl. Med. *6*, 232fs16. https://doi.org/10.1126/scitranslmed.3008558.
45. Nair, N.R., Sekhar, V.C., Nampoothiri, K.M., and Pandey, A. (2017). Biodegradation of Biopolymers. In Current Developments in Biotechnology and Bioengineering. [place unknown] (Elsevier), pp. 739–755. https://doi.org/10.1016/B978-0-444-63662-1.00032-4.
46. Bencherif, S.A., Srinivasan, A., Horkay, F., Hollinger, J.O., Matyjaszewski, K., and Washburn, N.R. (2008). Influence of the degree of methacrylation on hyaluronic acid hydrogels properties. Biomaterials *29*, 1739–1749. https://doi.org/10.1016/j.biomaterials.2007.11.047.
47. Jing, X., Wang, X.-Y., Mi, H.-Y., and Turng, L.-S. (2019). Stretchable gelatin/silver nanowires composite hydrogels for detecting

human motion. Mater. Lett. *237*, 53–56. https://doi.org/10.1016/j.matlet.2018.11.078.
48. Wu, L., Di Cio, S., Azevedo, H.S., and Gautrot, J.E. (2020). Photoconfigurable, Cell-Remodelable Disulfide Cross-linked Hyaluronic Acid Hydrogels. Biomacromolecules *21*, 4663–4672. https://doi.org/10.1021/acs.biomac.0c00603.
49. Kushibiki, T., Mayumi, Y., Nakayama, E., Azuma, R., Ojima, K., Horiguchi, A., and Ishihara, M. (2021). Photocrosslinked gelatin hydrogel improves wound healing and skin flap survival by the sustained release of basic fibroblast growth factor. Sci. Rep. *11*, 23094. https://doi.org/10.1038/s41598-021-02589-1.
50. Noshadi, I., Hong, S., Sullivan, K.E., Shirzaei Sani, E., Portillo-Lara, R., Tamayol, A., Shin, S.R., Gao, A.E., Stoppel, W.L., Black, L.D., III, et al. (2017). In vitro and in vivo analysis of visible light crosslinkable gelatin methacryloyl (GelMA) hydrogels. Biomater. Sci. *5*, 2093–2105. https://doi.org/10.1039/C7BM00110J.
51. Nicol, E. (2021). Photopolymerized Porous Hydrogels. Biomacromolecules *22*, 1325–1345. https://doi.org/10.1021/acs.biomac.0c01671.
52. Gipson, I.K., and Stepp, M.A. (2022). Anatomy and cell biology of the cornea, superficial limbus, and conjunctiva. In Albert and Jakobiec's Principles and Practice of Ophthalmology, pp. 3–30. https://doi.org/10.1007/978-3-030-42634-7_202.
53. Guo, Y., Wang, Y., Zhao, X., Li, X., Wang, Q., Zhong, W., Mequanint, K., Zhan, R., Xing, M., and Luo, G. (2021). Snake extract–laden hemostatic bioadhesive gel cross-linked by visible light. Sci. Adv. *7*, eabf9635. https://doi.org/10.1126/sciadv.abf9635.
54. Patel, S., and Tutchenko, L. (2019). The refractive index of the human cornea: A review. Cont. Lens Anterior Eye. *42*, 575–580. https://doi.org/10.1016/j.clae.2019.04.018.
55. Guan, X., Avci-Adali, M., Alarçin, E., Cheng, H., Kashaf, S.S., Li, Y., Chawla, A., Jang, H.L., and Khademhosseini, A. (2017). Development of hydrogels for regenerative engineering. Biotechnol. J. *12*, 1600394. https://doi.org/10.1002/biot.201600394.
56. Ulag, S., Uysal, E., Bedir, T., Sengor, M., Ekren, N., Ustundag, C.B., Midha, S., Kalaskar, D.M., and Gunduz, O. (2021). Recent developments and characterization techniques in 3D printing of corneal stroma tissue. Polym. Adv. Technol. *32*, 3287–3296. https://doi.org/10.1002/pat.5340.
57. Lang, N., Pereira, M.J., Lee, Y., Friehs, I., Vasilyev, N.V., Feins, E.N., Ablasser, K., O'Cearbhaill, E.D., Xu, C., Fabozzo, A., et al. (2014). A Blood-Resistant Surgical Glue for Minimally Invasive Repair of Vessels and Heart Defects. Sci. Transl. Med. *6*, 218ra6. https://doi.org/10.1126/scitranslmed.3006557.
58. Yao, M., Yaroslavsky, A., Henry, F.P., Redmond, R.W., and Kochevar, I.E. (2010). Phototoxicity is not associated with photochemical tissue bonding of skin. Lasers Surg. Med. *42*, 123–131. https://doi.org/10.1002/lsm.20869.
59. Scognamiglio, F., Travan, A., Borgogna, M., Donati, I., Marsich, E., Bosmans, J.W.A.M., Perge, L., Foulc, M.P., Bouvy, N.D., and Paoletti, S. (2016). Enhanced bioadhesivity of dopamine-functionalized polysaccharidic membranes for general surgery applications. Acta Biomater. *44*, 232–242. https://doi.org/10.1016/j.actbio.2016.08.017.
60. Zhou, D., Li, S., Pei, M., Yang, H., Gu, S., Tao, Y., Ye, D., Zhou, Y., Xu, W., and Xiao, P. (2020). Dopamine-Modified Hyaluronic Acid Hydrogel Adhesives with Fast-Forming and High Tissue Adhesion. ACS Appl. Mater. Interfaces *12*, 18225–18234. https://doi.org/10.1021/acsami.9b22120.
61. Barth, A. (2007). Infrared spectroscopy of proteins. Biochim. Biophys. Acta *1767*, 1073–1101. https://doi.org/10.1016/j.bbabio.2007.06.004.
62. Coates, J. (2000). Interpretation of Infrared Spectra, A Practical Approach. In Encyclopedia of Analytical Chemistry. [place unknown] (Wiley). https://doi.org/10.1002/9780470027318.a5606.
63. Delgado, A.H.S., and Young, A.M. (2021). Methacrylate peak determination and selection recommendations using ATR-FTIR to investigate polymerisation of dental methacrylate mixtures. PLoS One *16*, e0252999. https://doi.org/10.1371/journal.pone.0252999.
64. Yin, J., Singh, R.B., Al Karmi, R., Yung, A., Yu, M., and Dana, R. (2019). Outcomes of Cyanoacrylate Tissue Adhesive Application in Corneal Thinning and Perforation. Cornea *38*, 668–673. https://doi.org/10.1097/ICO.0000000000001919.
65. Yazdanpanah, G., Shen, X., Nguyen, T., Anwar, K.N., Jeon, O., Jiang, Y., Pachenari, M., Pan, Y., Shokuhfar, T., Rosenblatt, M.I., et al. (2022). A Light-Curable and Tunable Extracellular Matrix Hydrogel for In Situ Suture-Free Corneal Repair. Adv. Funct. Mater. *32*, 2113383. https://doi.org/10.1002/adfm.202113383.
66. Zhao, Y., Song, S., Ren, X., Zhang, J., Lin, Q., and Zhao, Y. (2022). Supramolecular Adhesive Hydrogels for Tissue Engineering Applications. Chem. Rev. *122*, 5604–5640. https://doi.org/10.1021/acs.chemrev.1c00815.
67. Bhattacharjee, P., and Ahearne, M. (2022). Silk fibroin based interpenetrating network hydrogel for corneal stromal regeneration. Int. J. Biol. Macromol. *223*, 583–594. https://doi.org/10.1016/j.ijbiomac.2022.11.021.
68. Yang, G., Espandar, L., Mamalis, N., and Prestwich, G.D. (2010). A cross-linked hyaluronan gel accelerates healing of corneal epithelial abrasion and alkali burn injuries in rabbits. Vet. Ophthalmol. *13*, 144–150. https://doi.org/10.1111/j.1463-5224.2010.00771.x.
69. Turley, E.A., Noble, P.W., and Bourguignon, L.Y.W. (2002). Signaling Properties of Hyaluronan Receptors. J. Biol. Chem. *277*, 4589–4592. https://doi.org/10.1074/jbc.R100038200.
70. Hao, Y., He, J., Ma, X., Feng, L., Zhu, M., Zhai, Y., Liu, Y., Ni, P., and Cheng, G. (2019). A fully degradable and photocrosslinked polysaccharide-polyphosphate hydrogel for tissue engineering. Carbohydr. Polym. *225*, 115257. https://doi.org/10.1016/j.carbpol.2019.115257.
71. Tankyo, Y., Harada, Y., Hiyama, T., Ohara, H., Mizukami, M., Okumichi, H., Hirooka, K., and Kiuchi, Y. (2022). Irreversible intraocular pressure elevation as a complication of MIRAgel scleral buckling. Am. J. Ophthalmol. Case Rep. *27*, 101583. https://doi.org/10.1016/j.ajoc.2022.101583.
72. Kong, B., Chen, Y., Liu, R., Liu, X., Liu, C., Shao, Z., Xiong, L., Liu, X., Sun, W., and Mi, S. (2020). Fiber reinforced GelMA hydrogel to induce the regeneration of corneal stroma. Nat. Commun. *11*, 1435. https://doi.org/10.1038/s41467-020-14887-9.
73. Pircher, M., Götzinger, E., Leitgeb, R., Fercher, A., and Hitzenberger, C. (2003). Measurement and imaging of water concentration in human cornea with differential absorption optical coherence tomography. Opt Express *11*, 2190–2197. https://doi.org/10.1364/oe.11.002190.
74. Barroso, I.A., Man, K., Hall, T.J., Robinson, T.E., Louth, S.E.T., Cox, S.C., and Ghag, A.K. (2022). Photocurable antimicrobial silk-based hydrogels for corneal repair. J. Biomed. Mater. Res. *110*, 1401–1415. https://doi.org/10.1002/jbm.a.37381.
75. Espana, E.M., and Birk, D.E. (2020). Composition, structure and function of the corneal stroma. Exp. Eye Res. *198*, 108137. https://doi.org/10.1016/j.exer.2020.108137.
76. Chae, J.J., Ambrose, W.M., Espinoza, F.A., Mulreany, D.G., Ng, S., Takezawa, T., Trexler, M.M., Schein, O.D., Chuck, R.S., and Elisseeff, J.H. (2015). Regeneration of corneal epithelium utilizing a collagen vitrigel membrane in rabbit models for corneal stromal wound and limbal stem cell deficiency. Acta Ophthalmol. *93*, e57–e66. https://doi.org/10.1111/aos.12503.
77. Rizwan, M., Peh, G.S.L., Ang, H.-P., Lwin, N.C., Adnan, K., Mehta, J.S., Tan, W.S., and Yim, E.K.F. (2017). Sequentially-crosslinked bioactive hydrogels as nano-patterned substrates with customizable stiffness and degradation for corneal tissue engineering applications. Biomaterials *120*, 139–154. https://doi.org/10.1016/j.biomaterials.2016.12.026.
78. Murugan, N.J., Vigran, H.J., Miller, K.A., Golding, A., Pham, Q.L., Sperry, M.M., Rasmussen-Ivey, C., Kane, A.W., Kaplan, D.L., and Levin, M. (2022). Acute multidrug delivery via a wearable bioreactor facilitates long-term limb regeneration and functional recovery in adult *Xenopus laevis*. Sci. Adv. *8*, eabj2164. https://doi.org/10.1126/sciadv.abj2164.
79. Schneider, C.A., Rasband, W.S., and Eliceiri, K.W. (2012). NIH Image to ImageJ: 25 years of image analysis. Nat. Methods *9*, 671–675. https://doi.org/10.1038/nmeth.2089.
80. Sampson, D.M., Ali, N., Au Yong, A., Jeewa, R., Rajgopal, S., Dutt, D.D.C.S., Mohamed, S., Mohamed, S., Hansen, A., Menghini, M., and Chen, F.K. (2020). RTVue XR AngioVue Optical Coherence Tomography Angiography Software Upgrade Impacts on Retinal Thickness and Vessel Density Measurements. Transl. Vis. Sci. Technol. *9*, 10. https://doi.org/10.1167/tvst.9.3.10.
81. Swift, M.L. (1997). GraphPad Prism, Data Analysis, and Scientific Graphing. J. Chem. Inf. Comput. Sci. *37*, 411–412. https://doi.org/10.1021/ci960402j.
82. Upadhyay, R.K., Mishra, A.K., and Kumar, A. (2020). Mechanical Degradation of 3D Printed PLA in Simulated Marine Environment. Surface. Interfac. *21*, 100778. https://doi.org/10.1016/j.surfin.2020.100778.
83. Percie du Sert, N., Ahluwalia, A., Alam, S., Avey, M.T., Baker, M., Browne, W.J., Clark, A., Cuthill, I.C., Dirnagl, U., Emerson, M., et al. (2020). Reporting animal research: Explanation and elaboration for the ARRIVE guidelines 2.0. PLoS Biol. *18*, e3000411. https://doi.org/10.1371/journal.pbio.3000411.
84. Sawicki, L.A., and Kloxin, A.M. (2014). Design of thiol–ene photoclick hydrogels using facile

techniques for cell culture applications. Biomater. Sci. *2*, 1612–1626. https://doi.org/10.1039/C4BM00187G.

85. Burroughs, M.C., Schloemer, T.H., Congreve, D.N., and Mai, D.J. (2023). Gelation Dynamics during Photo-Cross-Linking of Polymer Nanocomposite Hydrogels. ACS Polym. Au *3*, 217–227. https://doi.org/10.1021/acspolymersau.2c00051.

86. Raia, N.R., Jia, D., Ghezzi, C.E., Muthukumar, M., and Kaplan, D.L. (2020). Characterization of silk-hyaluronic acid composite hydrogels towards vitreous humor substitutes. Biomaterials *233*, 119729. https://doi.org/10.1016/j.biomaterials.2019.119729.

87. Fatehi, H., Ong, D.E.L., Yu, J., and Chang, I. (2023). The Effects of Particle Size Distribution and Moisture Variation on Mechanical Strength of Biopolymer-Treated Soil. Polymers *15*, 1549. https://doi.org/10.3390/polym15061549.

88. Ma, Y., Zhu, X., He, X., Lu, L., Zhu, J., and Zou, H. (2016). Corneal Thickness Profile and Associations in Chinese Children Aged 7 to 15 Years Old. PLoS One *11*, e0146847. https://doi.org/10.1371/journal.pone.0146847.

STAR★METHODS

KEY RESOURCES TABLE

REAGENT or RESOURCE	SOURCE	IDENTIFIER
Biological samples		
Cadaveric cornea tissues	Dr. Shroff's Charity Eye Hospital, New Delhi	20/12/22L (Left eye; extracted on 22/12/2020; 45 years old; male)
Porcine skin tissues	This paper	≥3 years old; ≥40 kg; male and female
Chemicals, peptides, and recombinant proteins		
Hyaluronic acid	Stanford Chemicals	HA-EP1
Gelatin	Nitta Gelatin Inc.	LS-250
Methacrylated hyaluronic acid	Blafar, Dublin	Lot: HAMA08022022
Thiolated gelatin	Blafar, Dublin	NBH3D31082022
Deuterium Oxide 99.9 atom % D	Sigma-Aldrich	Cat#151882 PCode 102569117
Ellman's Reagent	Thermo Fisher Scientific	Cat#22582
Cysteine-HCl	Thermo Fisher Scientific	Cat#44889
Saline	Fresenius Kabi	https://www.fresenius-kabi.com/in/products/ns
Eosin Y	Sigma-Aldrich	Cat#E4382
Triethanolamine	Sigma-Aldrich	Cat#90278
Phosphate Buffered Saline	Thermo Fisher Scientific	AM9625
MEM basal media	Gibco	Cat#11095080
Human Platelet Lysate	Life technologies	Cat#SER-HPL
Insulin Transferrin Selenium	Sigma-Aldrich	Cat#13146
Calcein AM	Invitrogen	Cat#C3099
Ethidium Homodimer-2	Invitrogen	Cat#E3599
Ketamine hydrochloride	Themis Medicare	6/UA/X/SC/P-2014
Xylazine	Indian Immunologicals Limited	30/MD/AP/2013/F/G
Proparacaine	Sunways (India) Pvt. Ltd.	G/1118A
Moxifloxacin	Sun Pharma	42/RR/TS/2016/F/G(L)
Fluorescein Stain	Madhu Instruments Pvt. Ltd.	MIPL/A4
Formalin solution, neutral Buffered, 10%	Sigma-Aldrich	HT5012
Hematoxylin	Sigma-Aldrich	H9627
Dibutyl phthalate Polystyrene Xylene	Sigma -Aldrich	44581
Experimental models: Organisms/strains		
New Zealand White Rabbits	Dabur Research Foundation, New Delhi, India	Oryctolagus cuniculus 8-10 weeks old; 1.8–2.0 kg, male.
Software and algorithms		
ImageJ	Schneider et al.[79]	https://imagej.nih.gov/ij/ RRID: SCR_003070
Avanti XR (OCT)	Sampson et al.[80]	Optovue Avanti https://www.ophthalmicmart.com/product/optovue-avanti/
GraphPad Prism Version 9	Swift[81]	https://www.graphpad.com RRID: SCR_000306
MTL32	Upadhyay et al.[82]	https://biss.in/basic-software.php

(*Continued on next page*)

Continued

REAGENT or RESOURCE	SOURCE	IDENTIFIER
Other		
Bruker Avance III HD 600 MHz	Bruker	https://www.ncbs.res.in/research-facilities/nmr-ins
LFS BiSS	BiSS, Instron	https://biss.in/single-column-lfs.php
MCR102 Rheometer	Anton Paar	https://www.anton-paar.com/in-en/products/details/rheometer-mcr-102-302-502/
OmniCure S1500	Excelitas Technologies	https://www.excelitas.com/product/omnicure-s1500-spot-uv-curing-system
Enspire Plate reader	Perkin Elmer	https://www.perkinelmer.com/category/microplate-readers
Digital refractometer	Hanna Instruments	HI-96800 https://hannainst.in/hi96800-digital-refractometer-for-refractive-index-and-brix
Vernier caliper	Sigma-Aldrich	Cat#Z503576
Stellaris Confocal Microscope	Leica Microsystems	https://www.leica-microsystems.com/products/confocal-microscopes/p/stellaris-8/
Slit-lamp biomicroscope	Appasamy India	https://www.appasamy.com/ophthalmology-optometery/dynamiq-slit-lamp
Pentacam	Oculus Pentacam	jhttps://www.pentacam.com/fileadmin/user_upload/pentacam.de/downloads/interpretations-leitfaden/interpretation_guideline_3rd_edition_0915.pdf Cat#70700
AS-OCT device (RTVue XR Avanti)	Optovue Inc.	https://www.oct-optovue.com/avanti/oct-avanti.html
HRT3 RCM	Heidelberg Engineering	https://business-lounge.heidelbergengineering.com/in/en/products/hrt3-rcm/hrt3-rcm/

RESOURCE AVAILABILITY

Lead contact

Further information and requests for resources and reagents should be directed to and will be fulfilled by the lead contact, Tuhin Bhowmick (tuhin@pandorumtechnologies.in).

Materials availability

This study did not generate new unique reagents.

Data and code availability

- All data reported in this paper will be shared by the lead contact upon request.
- This paper does not report original code.
- Any additional information required to reanalyze the data reported in this paper is available from the lead contact upon request.

EXPERIMENTAL MODEL AND STUDY PARTICIPANT DETAILS

Human cadaveric corneal rims

Human cadaveric corneal rims (Male, 20/12/22L) were obtained from Dr. Shroff's Charity Eye Hospital, New Delhi. Human corneal stromal cells were isolated from the limbal ring and incubated at 37°C in a 5% CO_2 incubator.[15]

Rabbits

The study was approved from Institutional animal ethics committee, Dabur Research Foundation, Uttar Pradesh, India. All surgical procedures were conducted under the supervision of a veterinarian and the animal care team as per the guidelines by the Association for Research in Vision and Ophthalmology (ARVO) regarding the use of animals in ophthalmic and vision research. Male New Zealand white rabbits approximately 8–10 weeks old weighing between 1.8 and 2.0 kg were used in the study. The study was performed in accordance to the ARRIVE Guidelines.[83]

Porcine skin tissues

The porcine skin tissues were purchased from an abattoir. Adult miniature pigs (≥3 years old; ≥40 kg; male and female) were used as donors.

METHOD DETAILS

Material characterization

^{1}H NMR analysis of biopolymers

^{1}H NMR was performed to measure the extent of functionalization of the biopolymers, using 800-MHz proton NMR in d_2O. The functionalized biopolymers, methacrylated hyaluronic acid (HA-MA) and thiolated gelatin (Gel-SH), were produced by Blafar Ltd., Dublin. Base hyaluronic acid (Stanford Chemicals, CA) polymer and gelatin (Sigma) were used as a reference for the identification of the specific peaks for functionalized products, i.e., HA-MA and Gel-SH.

Biochemical characterization

Ellman's assay was used to detect free sulfhydryl groups in the thiolated gelatin via colorimetric analysis using cysteine as standard. The assay was performed following the manufacturer's protocol. Briefly, Ellman's reagent (5,5′-dithio-bis-[2-nitrobenzoic acid]) was added to the sample solution and incubated at room temperature for 15 min, followed by measuring absorbance at 412 nm. The free sulfhydryl groups present in the sample were detected by comparing them with the standard curve prepared using cysteine standards in the reaction buffer.[84]

Preparation and characterization of kuragel

Preparation of kuragel

The functionalized biopolymers were mixed in concentration ratios, where HA-MA was 40–80 mg/mL and Gel-SH was between 50 and 140 mg/mL. The biopolymers were weighed and dissolved in normal saline (0.9% NaCl) by incubating at 37°C water bath for 30 min. Photo-initiator solution, comprising of eosin Y (0.05 mM) and triethanolamine (0.075% v/v) was added in 10 μL/mL of the biopolymer solution. This pre-gel solution was then dispensed on the molds or the corneal wound site in rabbits, and exposed to white light (Omnicure S1500) of 10 mW/cm^2, to obtain the hydrogel, which was termed as Kuragel.

The duration of light exposure to obtain Kuragel was assessed via change in storage modulus during the transition from pre-gel solution to the hydrogel form. The instrument used for this assessment was Rheometer (MCR102, Anton Paar).[85]

Optical characterization

Kuragels were prepared in 96 well plate in triplicate and transmittance to visible light was assessed by recording the spectra in a plate reader (Enspire, PerkinElmer). The obtained absorbance values were converted to transmittance by Beer Lambert's law, and plotted using saline as reference. Average transmittance was derived by averaging the values obtained for the complete visible spectra (400–700 nm).[86]

Refractive index was measured using digital refractometer (Hanna Instruments), where distilled water was used as blank.

Physio-chemical characterization

Kuragel discs were prepared in the molds of specified geometry (5 mm diameter and 1 mm height) and incubated in normal saline for assessing the swelling via change in weight and volume with time. The weight measurements were performed by soaking the excess saline from the Kuragel matrix and recording the weights at different time points. The swelling % by weight was measured using the relation: [(Wt-Wi)/Wi]×100. Where Wt is the weight recorded at different time points and Wi is the initial weight. Volumetric swelling was calculated by measuring the percentage increase in volume when the dimensions were measured using a Vernier caliper. The swelling % by volume was measured using the relation: [(Vt-Vi)/Vi]×100. Where Vt is the volume recorded at different time points and Vi is the initial volume.

Degradation rate of Kuragel was determined by incubating in 1X phosphate buffered saline (PBS) at ambient temperature under constant shaking (350 rpm) and measuring the change in weight with time. Other study groups included 1X PBS containing cocktail of enzymes (1 U/mL Hyaluronidase and 0.35 U/mL Collagenase I) and in the presence of encapsulated human corneal stromal stem cells (hCSCs). The degradation media was replenished every alternate day to avoid saturation and the hydrogel samples were retrieved at the predetermined time points and their weights were recorded after lyophilization for 24 h at −110°C. The degradation percentage was calculated using the relation: [(Wi-Wt)/Wt]×100. Where Wt is the dry weight at different time points and Wi is the initial dry weight recorded on the same day of sample preparation.

Cylindrical Kuragel were prepared as described above, and tested in a UTS instrument (BiSS mechanical tester) with parallel plate fixtures for compressive modulus assessment. The height and diameter of the Kuragel were recorded before loading into the instrument, then compressed at a rate of 1 mm/min up to a maximum of 50%, using a 44N load cell. The values for strain and load were recorded and the compressive modulus was calculated from the slope of stress versus strain curve, using linear region between 0.1 and 0.2 mm/mm strain.[82]

The adhesion strength of Kuragel to the biological tissue was assessed following the ASTM F2458-05 standards, using the method described elsewhere.[3] Briefly, the porcine skin tissues, purchased from a local butcher shop, were washed thoroughly to remove the oil and cut into 2.5 cm × 1.5 cm pieces. The skin tissue pieces were stuck to the glass slides using a commercially available superglue (fevikwik). An incision was made between the two adjacent glass slides and the skin tissues were kept 1 mm apart and the gap was filled in by 75 μL pre-gel solution followed by photo-crosslinking as described above. The assembly was incubated in 1X PBS for Kuragel equilibration (duration of

incubation was followed as per swelling studies) followed by adhesion testing in the BiSS UTS instrument. The glass slides were fixed in the wedge grips (without disturbing the alignment). The assembly was stretched at a rate of 1 mm/min until adhesive or cohesive failure was observed. Adhesion strength was calculated from the relation: (Maximum load/cross-sectional area) × 1000.

Attenuated Total Reflectance Fourier Transform Infrared (ATR-FTIR) spectroscopy (Spectrum Two, PerkinElmer), was used to identify the functional groups present in the biopolymers and the hydrogel.[87] The scanning range for ATR-FTIR analysis was 400–4000 cm^{-1}.

Biocompatibility assessment-*in vitro*

Cell encapsulation in hydrogel

Human corneal stromal cells (hCSCs), were isolated from cadaveric tissues as described earlier.[15] The passage 3 hCSCs were encapsulated in the density 1 million cells/mL of Kuragel. The cell suspension was mixed with the pre-gel solution and photo-crosslinked. The hCSCs encapsulated Kuragels were submerged in the complete culture media comprising of MEM basal media (Gibco, 11095080) with 5% HPL (Life technologies, SER-HPL) and 1X ITS (Sigma, 13146) (0.1 mL/10 mL media), and incubated at 37°C and 5% CO_2, with complete media change every 3rd day.

Cell viability assessment

The hCSC encapsulated Kuragel samples were removed from the culture at predetermined time points. The viability assessment media containing calcein acetoxymethyl (calcein-AM, 0.2 μg/mL) and ethidium homodimer (EthD-1, 2.5 μg/mL) (Invitrogen, Paisley, UK) prepared in the MEM media, was added to the samples and incubated for 15 min at 37°C. The samples were then observed under a confocal microscope (Stellaris, Leica microsystems) to mark the distribution of green alive cells and red stained dead cells.

In vivo efficacy of kuragel

Study design and approval

Male New Zealand white rabbits were used for the development and evaluation of mechanical injury to corneal epithelium and stroma through trephination of the right eye. The rabbits were 8–10 weeks old and weighed between 1.8 and 2.0 kg. The study received approval from Institutional Animal Ethics Committee and all surgical procedures were conducted under the supervision of a veterinarian and the animal care team at the Dabur Research Foundation, Ghaziabad, Uttar Pradesh, India. The handling of the animals adhered to the guidelines by the Association for Research in Vision and Ophthalmology (ARVO) regarding the use of animals in ophthalmic and vision research.

Corneal injury and kuragel treatment

Prior to the surgical procedure, the rabbits were given anesthesia through intramuscular injections of 30 mg/kg ketamine hydrochloride and 5 mg/kg xylazine. To ensure local anesthesia, a topical drop of proparacaine was applied to the right eye. For disease model generation, corneal tissue was precisely excavated using a guarded trephine with a diameter of 5 mm and a depth of 250 μm. Following injury, the eyes were imaged and Kuragel was applied.

The pre-gel solution of Kuragel was administered in the site of excavation and exposed to white light for 10 min for crosslinking, in 6 rabbits. Another six rabbits where wound was created, were left untreated (for reference as untreated negative control). Post-surgery management included, antibiotic eye drops (Moxifloxacin) four times a day for 7–10 days, until re-epithelization occurred. Bandage contact lens was applied as a precaution from accidental damage to the Kuragel layer. All the animals were monitored for a period of three months following the treatment.

Ophthalmic imaging of the rabbits

To track the progression of treatment, the animals were followed up by clinical photographs at regular intervals using the following techniques:

Slit Lamp: The rabbits were carefully positioned to ensure a clear view of the entire corneal frame, and images were captured using a slit-lamp biomicroscope (Appasamy, India) under four different conditions, diffuse light, fluorescein stain under cobalt blue light, green light and angle slit, allowing for a comprehensive examination of the cornea and neovascularization both in untreated and treated rabbit corneas. To track re-epithelialization, fluorescein stain was used and imaged under a cobalt blue light source.[50]

Anterior Segment Optical Coherence Tomography (AS-OCT): AS-OCT images can be used for measurement of corneal thickness and hyperreflectivity. In this study, an AS-OCT device (Optovue, Avanti RTVUE-XR) was employed to perform an anterior segment scan of the rabbit cornea. The OCT probe was positioned near the eye and central area was scanned. The images were processed using the integrated software (Avanti XR).[80] Images were further quantified for hyperreflectivity which is an indication of fibrosis using ImageJ,[79] NIH, software.

Pentacam. It is an advanced rotating Scheimpflug camera that provides information regarding corneal biomechanics, relating it to the densitometry (opacity score). It allows the evaluation of corneal properties at various diameters. The images obtained from pentacam were analyzed for opacity score at two annular diameters, 2 mm and 6 mm, using the built-in software.[88]

In vivo confocal microscopy (IVCM): IVCM was performed on rabbits at different time points to record the changes in the epithelium, subbasal nerve fibers, stroma, and endothelium, using Heidelberg HRT3 RCM. The density of all these layers was quantified using the inbuilt software.

Histological analysis

After a 90-day treatment with Kuragel, rabbits were euthanized using an overdose of ketamine and xylazine. Tissue samples from the cornea were collected from four groups: healthy rabbits (contralateral eye), diseased, wounded untreated, and 90 days after treatment with Kuragel. To prepare the tissues for histological analysis, they were first washed briefly with saline and then fixed in 10% neutral buffered formalin. For the histology process, the fixed sections were embedded in paraffin blocks. Subsequently, the sections were stained with Hematoxylin for 10 min and differentiated using 1% acid alcohol for 30 s. They were then rinsed in running tap water for 10 min and briefly washed in 95% alcohol for 20 s. To enhance the contrast, the sections were counterstained with Eosin Y for 30 s. Following this, the sections underwent dehydration using 95% alcohol and two changes of absolute alcohol, with each change lasting for 5 min. Finally, the sections were cleared using two changes of xylene for 5 min each and mounted using DPX (Dibutyl phthalate Polystyrene Xylene) mounting medium. The prepared sections were observed under light microscope.

QUANTIFICATION AND STATISTICAL ANALYSIS

Data were represented as mean values with standard deviation obtained using Graph Pad Prism 9.[81] Appropriate non-parametric one-way ANOVA tests were performed for the assessment of significance between different time points, where p value ≤ 0.05 was defined as threshold. Significant difference between the standard deviations of the means was measured using Brown-Forsythe and Barlett's tests. A minimum number of replicates was three for each test, represented as 'n' values, unless described otherwise in corresponding methods and figure legends.